Sedimentological and geochronological constraints on the Carboniferous evolution of central Inner Mongolia, southeastern Central Asian Orogenic Belt: Inland sea deposition in a post-orogenic setting

Pan Zhao, Bei Xu, Qinlong Tong, Yan Chen, Michel Faure

Sedimentological and geochronological constraints on the Carboniferous evolution of central Inner Mongolia, southeastern Central Asian Orogenic Belt: inland sea deposition in a post-orogenic setting

Pan Zhao[a,b] , Bei Xu[a*], Qinlong Tong[c], Yan Chen[b,d,e], Michel Faure[b,d,e]

[a] Key Laboratory of Orogenic Belts and Crustal Evolution, Ministry of Education, Peking University, Beijing, 100871, China

[b] Université d'Orléans, ISTO, UMR 7327, 45071 Orléans, France

[c] National Key Laboratory of Remote Sensing Information and Image Analysis Technology, Beijing Research Institute of Uranium Geology, Beijing 100029, China

[d] CNRS/INSU, ISTO, UMR 7327, 45071 Orléans, France

[e] BRGM, ISTO, UMR 7327, BP 36009, 45060 Orléans, France

[*]Corresponding author E-mail address: bxu@pku.edu.cn

Abstract

Sedimentological and geochronological analyses were performed on Carboniferous strata from central Inner Mongolia (China) to determine the tectonic setting of the southeastern Central Asian Orogenic Belt (CAOB). Sedimentological analyses indicate that the widespread Late Carboniferous strata in central Inner Mongolia were dominated by shallow marine clastic-carbonate deposition with basal conglomerate above the Precambrian basement and Early Paleozoic orogenic belts. Based on lithological comparison and fossil similarity, five sedimentary stages were

used to represent the Carboniferous deposition. The depositional stages include, from bottom to top, 1) basal molassic, 2) first carbonate platform, 3) terrigenous with coeval intraplate volcanism, 4) second carbonate platform, and 5) post-carbonate terrigenous. These five stages provide evidence for un extensive transgression in central Inner Mongolia during the Late Carboniferous. Detrital zircon geochronological studies from five samples yielded five main age populations: ~310 Ma, ~350 Ma, 400-450 Ma, 800-1200 Ma and some Meso-Proterozoic to Neoarchean grains. The detrital zircon geochronological studies indicate that the provenances for these Late Carboniferous strata were mainly local magmatic rocks (Early Paleozoic arc magmatic rocks and Carboniferous intrusions) with subordinate input of Precambrian basement. Combining our sedimentological and provenance analyses with previous fossil comparison and paleomagnetic reconstruction, an inland sea was perceived to be as the main paleogeographic feature for central Inner Mongolia during the Late Carboniferous. The inland sea developed on a welded continent after the collision between North China Craton and its northern blocks.

Key words: Central Asian Orogenic Belt; Central Inner Mongolia; Carboniferous; Sedimentary; Detrital zircon

1 Introduction

The Central Asian Orogenic Belt (CAOB), also referred to as the Altaid tectonic collage, is considered to be the largest Phanerozoic accretionary orogenic belt in the world and has attracted attention and intensive research for several decades (Sengör et

al., 1993; Jahn et al., 2000; Windley et al., 2007; Xiao et al., 2010; Wilhem et al., 2012; Choulet et al., 2013; Zhou and Wilde, 2013; Kröner et al., 2014; Xiao and Santosh, 2014). The CAOB records long-term evolution of the Paleo-Asian Ocean from the Neoproterozoic (Khain et al., 2002) to the Late Paleozoic (Sengör et al., 1993; Xiao et al., 2003; 2009; Wilhem et al., 2012; Xu et al., 2013), and represents the most important place for Phanerozoic crust growth, producing abundant juvenile crust with positive epsilon Nd and Hf (Han et al., 1997; Jahn et al., 2000; 2004; Chen et al., 2009). The CAOB formed by complicated subduction-accretion processes, with various fragments including microcontinents, island arcs, ophiolite complexes, seamounts, oceanic plateaus, and accretionary prisms (Windley et al., 2007; Safonova et al., 2011; Choulet et al., 2012; Wilhem et al., 2012; Safonofa and Santosh, 2014). After the accretion and collision, the former united fragments re-activated, with intra-plate magmatism and deposition occurring in the extensional zones (Tang, 1990; Hong et al., 1994; Zhang et al., 2008; Yarmolyuk et al., 2008; Jahn et al., 2009; Yuan et al., 2010; Han et al., 2011; Chen et al., 2012; Yu et al., 2013). In this case study, we chose the north margin of North China Craton (NCC), located in the southeast of CAOB, to decipher the transition between accretion and post-accretional extension.

The central part of Inner Mongolia (China), located at the north of NCC, represents a key area for studying the evolution between NCC and the Siberian Craton (SIB), who were separated by the Paleo-Asian Ocean (PAO) (Fig. 1a; Zonenshain et al., 1990; Windley et al., 2007; Xiao et al., 2010). The PAO was first introduced by Zonenshain et al. (1990). Its closure recorded the successive accretion of microblocks

and magmatic arcs to the north margin of NCC and south margin of SIB, respectively (Didenko et al., 1994; Dovretsov et al., 2003; Safonova, 2009; Xiao et al., 2010). Debates over the closure of PAO between NCC and SIB have lasted over decades, especially on the position and timing of the final closure. Based on two sub-parallel ophiolitic mélanges and relative unconformities, Tang (1990) considered that PAO closed in the Late Devonian. Xu et al. (2013; 2014) improved this model and suggested a microblock called Songliao-Hunshandake Block (SHB) exists between NCC and the Airgin Sum-Xilinhot-Xing'an Block (AXXB), which separates PAO into the southern and northern branches. The southern branch closed in the Late Silurian by the Southern Orogen, while the northern branch closed in the Late Devonian by the Northern Orogen (Xu et al., 2013; 2014). Nevertheless, Jian et al. (2008) considered that these two orogenic belts were caused by continent-arc collision. The subduction of PAO beneath NCC restarted in the Late Carboniferous, forming intra-oceanic arc–trench related magmatic rocks, with the final closure of PAO occurring in the Late Permian (Jian et al., 2010). However, many authors argued that PAO lasted for the whole Paleozoic until the latest Permian final collision along the Solonker suture zone based mainly on geochronological and geochemical studies of Carboniferous-Permian granitoids and mafic-ultramafic intrusions (Chen et al., 2000; Xiao et al., 2003; Zhang et al., 2009; Liu et al., 2013). Li (2006) even considered that the final collision did not occur until the Early Triassic along the Xar Moron fault according to the Early Triassic syntectonic granites.

The key for understanding the contradiction of these models and revealing the

tectonic history of central Inner Mongolia should be found in the Carboniferous rocks because they connect the two disputed closing times, the Late Devonian and Late Permian, and the Carboniferous rocks crop out in all tectonic blocks recognized in Inner Mongolia. Because only a few Carboniferous magmatic rocks are exposed in central Inner Mongolia, previous studies resulted in the opposite interpretation of geochemical affinities and relationship with country rocks and did not allow geologists to reach a consensus about the Carboniferous tectonics (Bao et al., 2007; Zhang et al., 2007; 2009a; Liu et al., 2008; Tang et al., 2011; Zhang et al., 2012; Liu et al., 2013). Fortunately, Carboniferous sedimentary strata are widespread in Inner Mongolia, and they may provide a good opportunity to study the Carboniferous sedimentary-tectonic environment and to understand its geodynamic implication. Meanwhile, sedimentological studies are relatively short in this area though they may provide fundamental information on the tectonic evolution. Only Mueller et al. (1991) previously compared sedimentological data for the Late Paleozoic strata in Inner Mongolia, while others either focused on the Late Paleozoic strata in a local region (Jiang et al., 1995a,b; Xu and Chen et al., 1997) or the Mesozoic rift basins in southern Mongolia and Inner Mongolia (Hendrix et al., 1996; Graham et al., 2001; Meng, 2003; Johnson, 2004). Moreover, most previous sedimentological studies consisted of reviews that do not include enough first-hand sedimentary data. Hence, in this paper we present new sedimentological analyses of major outcrops of Carboniferous strata, the corresponding detrital zircon results from five main localities in central Inner Mongolia (Fig. 1), and try to interpret their tectonic

implications.

2 Tectonic frameworks

Central Inner Mongolia consists of several units, namely Airgin Sum-Xilinhot-Xing'an Block (AXXB), Songliao-Hunshandake Block (SHB), and north margin of NCC from north to south (Fig. 1b). These three blocks are separated by the Late Devonian Northern Orogen and Late Silurian-Early Devonian Southern Orogen (Tang, 1990; Jian et al., 2008; Xu et al., 2013; Fig. 1b).

The AXXB, also called Hutag Uul Block in southern Mongolia (Badarch et al., 2002), extends through Airgin Sum-Sunidzuoqi-Xilinhot area to Xing'an area in northeastern China (Wu et al., 2007; Xu et al., 2014). The Precambrian basement is mainly composed of strongly deformed and metamorphosed Neoproterozoic mica schist, meta-volcanic rocks, meta-sandstone and marble (IMBGMR, 1991; Badarch et al., 2002). Two U-Pb ages of 952±8 Ma and 916±16 Ma have been reported for the Hutag Uul Block (Wang et al., 2001; Yarmolyuk et al., 2005). Recently, Mesoproterozoic gneissic granites were identified from the Sunidzuoqi area with U-Pb age of 1516±31 Ma and 1390±17 Ma, indicating the existence of Precambrian basement in this region (Sun et al., 2013). Although new detrital zircon studies of the Xilin Gol complex show some Early Paleozoic component and was considered to represent the Early Paleozoic deposition (Chen et al., 2009; Xue et al., 2009; Li et al., 2010), further study divided the Xilin Gol complex into Precambrian supercrustal rocks and Paleozoic intrusion (Ge et al., 2011).

The SHB is located between two orogenic belts (Fig. 1b). The basement of SHB is made of Paleo- and Neo-proterozoic granitic rocks, which has been well documented from the eastern part of this block (Zhang et al., 2012; Xu et al., in press). However, for the western part (our study area), evidence for a Precambrian basement is rare. The Lower Paleozoic Ondor Sum Group was considered as the sedimentary cover of this block, which was deformed during twice orogenic events (Xu et al., 2013). Detrital zircon dating from the mica schist of Ondor Sum Group also provides an abundance of data for the Paleo- and Neo-proterozoic (author's unpublished data).

Both the Southern Orogen and Northern Orogen consist of Early Paleozoic arc magmatic rocks, ophiolitic mélange, and blueschist facies metamorphic rocks. The opposite direction of PAO subduction during the Early Paleozoic produced Bainaimiao Arc at ca. 500-410 Ma to the south and Baolidao Arc at ca. 500-420 Ma to the north (Chen et al., 2000; Jian et al., 2008; Zhang et al., 2013). Ordovician volcanic rocks and Silurian flysch were deposited near to the two magmatic arcs, forming a typical oceanic subduction related rock assemblage (Xu et al., 2013). Meanwhile, blueschist facies metamorphic rocks were identified from both orogenic belts (Tang and Yan, 1993; Xu et al., 2001; De Jong et al., 2006).

After the orogenic events, conglomerates and sandstones of the Upper Silurian-Lower Devonian Xibiehe Formation and Upper Devonian Seribayanaobao Formation unconformably overlay the ophiolitic mélange, arc magmatic rocks and Precambrian basement along the Southern and Northern orogens, respectively

(Zhang et al., 2010; Xu et al., 2013). These formations were interpreted as molassic deposits that formed the first sedimentary cover after the orogenic events (Zhang et al., 2010; Xu et al., 2013).

Different from the Devonian molassic deposition, which developed along orogenic belts, the Carboniferous-Permian strata are widespread in central Inner Mongolia (IMBGMR, 1991; Mueller et al., 1991). The Carboniferous strata consist of ca. 1500~3000 m-thick series of limestone, conglomerate, and sandstone with subordinate volcanic rocks. The abundant fossils (e.g., coral, brachiopoda, fusulinids) found in these Carboniferous strata indicate a predominant shallow marine depositional environment (IMBGMR, 1991). The Early Permian Dashizhai Formation is characterized by bimodal volcanic rocks (Zhang et al., 2008). In later times, the Middle Permian Zhesi Formation, famous for its Zhesi fauna, was deposited as shallow marine limestone and sandstone (e.g. Wang et al., 2004). The Upper Permian deposits of ca. 4000 m-thick terrestrial conglomerate and shale dominate the whole region (IMBGMR, 1991; Mueller et al., 1991).

3. Petrography and sedimentology of Carboniferous strata

The Carboniferous strata, especially the Late Carboniferous ones, are widespread in central Inner Mongolia and crop out in three blocks of this region (Fig. 1b). Along the Northern Orogen, they conformably covered the Late Devonian molassic deposits (Xu et al., 2013), while they unconformably covered the Late Silurian-Early Devonian molassic deposits along the Southern Orogen (IMBGMR, 1991). We

selected five typical sections for sedimentological studies, positions of which are marked in Fig. 1b. The stratigraphic framework in central Inner Mongolia has been constrained by several geological mapping projects and paleontological studies (Li et al., 1996 and references therein)that provide a control on the timing and duration of the Carboniferous sedimentation. Relative chronostratigraphic framework for each locality is illustrated in Fig. 2, including the Early Carboniferous deposits that can only be identified in Sunidzuoqi and Aohanqi. However, the Late Carboniferous strata, represented by Benbatu and Amushan Formations, or Jiadaogou and Jiujuzi formations, are widespread in central Inner Mongolia (Fig. 2). Their detailed lithofacies and sedimentary environment will be discussed below.

3.1 Sunidzuoqi section

The Sunidzuoqi section (S-1 in Fig. 1b), located along the Northern Orogen, developed above the Late Devonian molassic conglomerate-sandstone, which unconformably overlies the ophiolitic mélange (Xu and Chen, 1997; Xu et al., 2013). The Sunidzuoqi section is composed of, from bottom to top, Lower Carboniferous Gouhudag and Nomgenhudag Formations, and Upper Carboniferous Benbatu and Amushan Formations (Fig. 2).

The 886 m-thick Gouhudag Formation is composed of purple lithic sandstone in the lower part (Fig. 3a), yellowish sandstone in the upper part (Fig. 3b), and 40 m-thick limestone on the top. Inclined beddings can be observed in the sandstone part (Fig. 3b). The clastic materials, especially for the lower lithic sandstone, are mainly composed of polycrystalline lithic fragments that originated from magmatic rocks and

imply a possible provenance from a nearby orogenic belt. The overlying 391 m thick Nomgenhudag Formation is characterized by sandstone interbedded with siltstone in the lower part, and laminated mudstone in the upper part (Fig. 3). This formation yields abundant sedimentary structures, such as wavy bedding (Fig. 3c), bedding-parallel mud nodules (Fig. 3d), inclined bedding (Fig. 3e) in sandstone, and flat bedding (Fig. 3f) and lamina in siltstone and mudstone. All sedimentary structures indicate an alternation of turbulent and stable hydrodynamism.

Different from the Lower Carboniferous terrigenous sediments, the Upper Carboniferous Benbatu and Amushan Formations are mainly composed of marine limestone with a few siltstone interlayers (Fig. 3). The base of Benbatu Formation is marked by the brecciated limestone with sandstone breccias of 2-10 cm in length (Fig. 3g), indicating an erosional basal contact. Following that, 0.2-1 m-thick beds of sparite and 0.1-0.5 m-thick beds of bioclastic limestone (Fig. 3h) are interbedded, with fossils of corals, fusulinids and crinoids. The upper part of the Benbatu Formation comprises 762 m-thick of rhyolite, dacite, basalt and tuff, with bimodal geochemical features consistent with an extensional setting (Tang et al., 2011). Following the volcanic rocks, the basal limestone of the Amushan Formation contains pebbles of underlying volcanic rocks, also indicating an erosional contact, followed by interbedded sandy limestone, bioclastic limestone and sparite with fusulinids and crinoids (Fig. 3). These two limestone-dominated strata represent carbonate platform deposition.

3.2 Ondor Sum area

The Ondor Sum section (S-2 in Fig. 1b), located along the Southern Orogen (Fig. 1b), is composed of the Upper Carboniferous Hailasiamu, Benbatu and Amushan Formations that unconformably cover the Lower Devonian Xibiehe Formation (Fig. 2).

The 380 m-thick Hailasiamu Formation is composed of pebble bearing quartz sandstone interbedded with black siltstone in the lower part (Fig. 4a), and black siltstone in the upper part (Fig. 4b). Abundant plant fossils can be found in several black siltstone layers (Fig. 4c). The whole sequence represents a transition from fluvial to lacustrine facies deposition. The Benbatu Formation is not well developed in this area with only 136 m-thick fusulinid-bearing limestone (Fig. 4) that is representative of carbonate platform deposition.

The 2590 m-thick Amushan Formation can be divided into three continuous sequences according to rock types. The lower clastic sequence is composed of massive coarse sandstone with large cross bedding in the lower part (Fig. 4d), followed by sandstone interbedded with mudstone in the upper part (Fig. 4e), representing an upward fining sequence from tidal flat with high water energy to littoral sea. The middle carbonate sequence consists mainly of massive sparite and bioclastic limestone with abundant fusulinids (Figs. 4f and 4g), which indicate platform deposition. Several sandstone and pebbly sandstone layers that indicate the input of terrigenous materials can be found within the limestone sequence (Fig. 4h). The upper clastic sequence is composed of quartz sandstone, siltstone, and limestone with important lateral variations.

3.3 Aerbaolage area

The Aerbaolage section (S-3 in Fig. 1b), located to the north of the Northern Orogen (Fig. 1b), is composed of the Upper Carboniferous Benbatu and Amushan Formations (Fig. 2).

The Benbatu Formation starts with a 45 m-thick basal conglomerate, but the underlying formation is unknown. The 2-20 cm diameter gravels are rounded to sub-rounded, poorly sorted, and composed of felsic volcanic rocks (Fig. 5a). These features indicate an alluvial facies with rapid proximal accumulation that can be considered as molassic deposition. The subsequent 72 m-thick lithic coarse sandstone consists mainly of low mature fragments, such as lithic and feldspar, also indicating a proximal deposition. The 765 m-thick limestone is thick bedded, in which shallow marine fossils including corals (Fig. 5b), brachiopods, and crinoids, dated to the Upper Carboniferous, have been found (IMBGMR, 1991). The limestone was later covered by yellow siltstone (Fig. 5c). In its entirety, the Benbatu Formation represents a fining upward sequence from basal conglomerate to littoral carbonate and clastic deposition.

Overlying the Benbatu Formation, the lower part of the Amushan Formation is composed of tuff and siltstone with horizontal beddings (Fig. 5d), which are interbedded with quartz sandstone. Wave beddings and soft sediment deformation can be observed (Fig. 5e), indicating a turbulent depositional environment. The middle part consists of mainly massive coarse-grained sandstone interbedded with sandstone (Fig. 5f) with cross beddings (Fig. 5g) that are representative of a near shore strongly

turbulent environment with sufficient terrigenous material input. The upper part of this formation is composed of thick layered (1-3 m) sandstone interbedded with thin-medium layered (5-30 cm) black siltstone-mudstone (Fig. 5h), which may represent periodic sea level change. Wave beddings and horizontal beddings in siltstone and mudstone represent transgression and relatively low water energy. While thick-layered sandstone and plant debris indicate regression and a turbulent water environment. Within the top limestone, abundant shallow marine fossils (e.g. brachiopods, corals and lamellibranches) have been observed (IMBGMR, 1991).

3.4 West-Ujimqin area

The West-Ujimqin section (S-4 in Fig. 1b), located along the Northern Orogen (Fig. 1b), consists of the Upper Carboniferous Benbatu and Amushan Formations (Fig. 2).

The 490 m-thick Benbatu Formation is composed of conglomerate at the bottom, several fining upward cycles in the lower part and limestone in the upper part. The basal conglomerate represents a regional unconformity, which covered the underlying metamorphic basement (Bao et al., 2006). The fining upward cycles contain conglomerate-coarse sandstone-sandstone at the bottom and sandstone-siltstone-mudstone at the top, which represent a fining upward sequence (Fig. 6a) and a gradual transgression (Bao et al., 2006). Inclined beddings can be found within the coarse quartz-sandstone layers (Fig. 6b), showing a turbulent environment. The blue thin-layered limestone contains numerous brecciated intraclasts (Fig. 6c) and fossil debris with soft sediment structures, also indicating high water energy.

Overlying the Benbatu Formation, the basal part of the Amushan Formation is a conglomerate with pebbles of the underlying sandstone and limestone (Fig. 6d) that indicates an erosional contact and may represent a regional regression. After the 70-m-thick interbedded sandstone and limestone, carbonate deposits dominate the lower sequence with shallow marine fossils (e.g., corals, fusulinids, and crinoids) that represent a stable platform deposition. The upper part of this carbonate sequence is composed of intraclast limestone and sandy intraclast limestone (Fig. 6e) that are indicative of high energy mid-ramp depositional environments (Burchette and Wright, 1992). The upper clastic sequence is composed of conglomerate at the bottom, followed by sandstone and siltstone. Inclined beddings and soft sediment deformation are pervasive in the sandstone layers (Figs. 6f and 6g) with plant fossil debris, all of which indicate near shore deposition. Then, mud breccias are found within the low maturity yellow coarse feldspar-quartz sandstone (Fig. 6h), indicating a near shore deposition environment, possibly affected by storms.

3.5 Aohanqi area

The Aohanqi section (S-5 in Fig. 1b), located to the south of the Southern Orogen (Fig. 1b), is composed of the Lower Carboniferous Houfangshengou Formation and Upper Carboniferous Jiadaogou and Jiujuzi Formations (Fig. 2).

The 1230 m-thick Houfangshengou Formation is composed of blue-grey thick-bedded limestone (0.3-1.5 m, Fig. 7a) with thin layers of siltstone interstratified in the upper part (Fig. 7b). The striking feature of this sequence is the abundance of shallow marine fossils, such as coral, crinoids, fusulinids and brachiopoda (Fig. 7c).

The massive beds and abundant corals represent reef limestone deposited on a carbonate platform (e.g. Coniglio and Dix, 1992). On the top of this formation, nodular limestone shows sea level fall, and significant energy fluctuations.

The 1054 m-thick Jiadaogou Formation is composed of 10-20 cm-thick bedded limestone interbedded with sandstone and siltstone (Figs. 7d and 7e). The most important difference from the underlying Houfangshengou Formation is the significant increase of siliciclastic materials. In addition, brachiopodas, instead of corals, are the main fossils in this formation.

The Jiujuzi Formation is 700 m thick interbedded with quartz sandstone and plant fossil-bearing black mudstone (Fig. 7). From bottom to top, the thickness of black laminated mudstone increases from centimeter to meter scale, showing a thinning upward sequence. The quartz sandstone is medium- to thick-bedded with graded bedding (Fig. 7f). The angular to subangular quartz grains are 2-5 mm in diameter and range from grain supported at the bottom to matrix supported at the top (Fig. 7f). The black shale is laminated but homogeneous with abundant burrows and plant fossils (Figs. 7g and 7h). The basal contact with quartz sandstone is sharp, whereas the upper contact is mainly erosive and indicates a high energy environment when the coarse sandstone was deposited. The quartz sandstone-shale sequence of the Jiujuzi Formation is interpreted as a meandering fluvial deposit based on its thinning upward quartz sandstone-shale sequence, and abundance of borrows and wood fossils (Hendrix et al., 1996; Prothero and Schwab, 2003). The quartz sandstone layers were deposited during a flood period. The high energy streams brought coarse grains that

cut the former black shales and formed an erosive contact. As the flood period weakened, the amount of fine-grained material increased and graded beddings developed in the sandstone. After the flood, organic rich clay-sized particles with mollusk burrows and plant materials were deposited on the floodplain to form black shale.

4. Geochronological control of Carboniferous deposits

Detrital zircon U-Pb dating was carried out on sandstone samples from each locality (Fig. 1b) to determine the age and provenance of these Carboniferous strata. Detailed information and locations for each sample are given in Table 1 and Fig. 1b, respectively.

4.1 Analytical methods

Zircons were separated using heavy liquid and magnetic techniques, and purified by handpicking under the binocular microscope. After photographing under reflected and transmitted light, Cathodoluminescence (CL) images were obtained using a Quanta 200 FEG Scan Electron Microscope in the Peking University in order to investigate the internal structure and choose target sites for U-Pb analyses. CL images of typical zircons are presented in Fig. 8. The U-Pb ages were determined by Laser ablation-inductively coupled plasma-mass spectrometry (LA-ICP-MS) at the Key Laboratory of Orogen and Crust Evolution, Peking University. The instrument couples a quadrupole ICP-MS (Agilient 7500c) and 193-nm ArF Excimer laser (COMPexPro 102, Coherent, DE) with the automatic positioning system. Calibrations

for the zircon analyses were carried out using NIST 610 glass as an external standard and Si as internal standard. U-Pb isotope fractionation effects were corrected using zircon Plesovice (337 Ma) as external standard. Zircon standard 91500 is also used as a secondary standard to supervise the deviation of age measurement/calculation. Isotopic ratios and element concentrations of zircons were calculated using GLITTER (ver. 4.4.2, Macquarie University). Concordia ages and diagrams were obtained using Isoplot/Ex (3.0) (Ludwig, 2003). The common lead was corrected using LA-ICP-MS Common Lead Correction (ver. 3.15), following the method of Andersen (2002). The analytical data are presented on U-Pb Concordia diagrams with 2σ errors. The mean ages are weighted means at 95% confidence levels (Ludwig, 2003).

4.2 Detrital zircon dating results

4.2.1 Lower Carboniferous sandstone from Sunidzuoqi (#090711-31)

This sample was collected from the upper part of the Lower Carboniferous Nomgenhudag Formation. The zircon grains are euhedral to subhedral in shape, with 30-70 μm in width and 50-90 μm in length. Most grains show oscillatory zoning and some old grains show bright to grey cores with weak oscillatory growth zoning (Fig. 8). In total, 75 grains were analyzed with 69 concordant results (<10% discordance and most <5%). The Th/U ratios ranged from 0.23 to 1.35, which are characteristic of an igneous origin. The 69 concordant analyses yielded apparent ages ranging from 328±4 Ma to 2894±27 Ma (Supplementary Table 1) and could be grouped into two main age populations: 328-503 Ma (n=53) with main peak at 430 Ma and secondary peak at 348 Ma; 705-1313 Ma (n=13) without peak age (Fig. 9). In addition, one

Archean and two Paleoproterozoic grains yielded $^{207}Pb/^{206}Pb$ ages of 2894±27 Ma, 1631±31 Ma and 1581±106Ma, respectively (Supplementary Table 1).

4.2.2 Upper Carboniferous sandstone from Ondor Sum (#100624-25)

The sample was collected from the lower part of the Upper Carboniferous Amushan Formation. The zircon grains are euhedral to subhedral, ranging from 40-60 μm in width and 50-100 μm in length with oscillatory growth zoning (Fig. 8). A total of 75 zircons were analyzed and 71 of them were concordant. The Th/U ratios range from 0.37 to 1.99, indicating a magmatic origin. Among the 71 concordant analyses, 70 of them yielded apparent ages ranging from 403±5 Ma to 496±5 Ma, with a peak age of 443 Ma (Fig. 9). Only one grain yielded an age of 1136±29 Ma (Supplementary Table 1).

4.2.3 Upper Carboniferous sandstone from Aerbaolage (#130615-04)

The sample was collected from the lower part of the Upper Carboniferous Benbatu Formation. The zircon grains are euhedral, ranging from 40-60 μm in width and 80-200 μm in length with well developed oscillatory growth zoning (Fig. 8). Seventy-three of the total 75 analyzed zircons were concordant. The Th/U ratios ranged from 0.34 to 1.34, indicating magmatic origin. The 73 concordant analyses showed a population with a narrow range of ages (from 283±3 Ma to 353±5 Ma) and a peak age of 307 Ma (Fig. 9; Supplementary Table 1).

4.2.4 Upper Carboniferous sandstone from West-Ujimqin (#100701-23)

The sample was collected from the lower part of the Upper Carboniferous Amushan Formation. The zircon grains are euhedral to subhedral, ranging from 40-60

μm in width and 50-150 μm in length with fine-scale oscillatory growth zoning (Fig. 8). Seventy of the total 75 analyzed zircons were concordant, with the Th/U ratios ranging from 0.15 to 1.41, indicating a magmatic origin. The 70 concordant analyses yielded apparent ages ranging from 283±3 Ma to 2450±9 Ma (Supplementary Table 1) and exhibited one main age population of 283-498 Ma (n=61), with age peaks of 313 Ma and 412 Ma (Fig. 9). In addition, nine Precambrian grains yielded ages from 545±5 Ma to 2450±9 Ma without peak age (Fig. 9).

4.2.5 Upper Carboniferous sandstone from Aohanqi (#130622-01)

The sample was collected from the lower part of the Upper Carboniferous Jiadaogou Formation. The zircon grains are euhedral to subhedral, ranging from 40-80 μm in width and 50-150 μm in length with well-developed oscillatory growth zoning (Fig. 8). Analyses for 73 of 75 grains were valid and concordant. The Th/U ratios range from 0.15 to 1.72, indicating magmatic origin. The concordant zircons yielded apparent ages that ranged from 305±4 Ma to 2559±17 Ma (Supplementary Table 1) and belonged to one main age population of 305-483 Ma (n=70), having an age peak of 384 Ma (Fig. 9). In addition, three Precambrian grains yielded ages at 2458±10 Ma, 2488±10 Ma, and 2559±17 Ma (Fig. 9).

5. Discussion

5.1 Stratigraphic correlation and basin paleogeography

The sedimentological analyses demonstrate a basal contact of most of the Late Carboniferous strata with the underlying Precambrian basement and Early Paleozoic arc magmatic rocks. A composite lithostratigraphic correlation chart (illustrated in Fig.

10) can be used to represent the five main sedimentary stages of the Carboniferous strata in central Inner Mongolia based on the similarities in lithologic assemblages, fossils and detrital zircon U-Pb dating results.

5.1.1 Basal molassic deposition

Two unconformities have been identified along both the southern and northern orogens, which postdated these two orogenic events before the Late Silurian and Late Devonian, respectively (Tang, 1990; Xu et al., 2013). Late Silurian- Early Devonian molassic sediments of the Xibiehe Formation unconformbly covered the metamorphic basement and ophiolitic mélange along the Southern Orogen (Tang, 1990; Li et al., 1996; Zhang et al., 2010). After that, the whole region along the Southern Orogen became a subaerial environment without sediments until the Late Carboniferous. For the Northern Orogen, the ophiolitic mélange was unconformably covered by the Late Devonian conglomerate of the Seribayanaobao Formation, identified from the Sunidzuoqi area (Fig. 10a; Xu et al., 2013). The sequence, starting with the Late Devonian terrestrial molassic conglomerate, became finer upward into the Early Carboniferous littoral terrigenous lithic sandstone and siltstone (Figs. 3 and 10).

At the beginning of the Late Carboniferous, an extensive transgression occurred after the Silurian-Devonian orogenic events (IMBGMR, 1991), and produced the molassic-like deposit at the bottom of Late Carboniferous strata in several localities of central Inner Mongolia (e.g. Ondor Sum, Aerbaolag, and West-Ujimqin) as shown in Fig. 10. In the Ondor Sum area, the lowermost Hailasiamu Formation, which unconformably covered the Xibiehe Formation (IMBGR, 1976), is mainly composed

of fluvial coarse quartz-sandstone and plant fossils bearing lacustrine black siltstone, indicating a terrestrial deposition (Fig. 10). In the Aerbaolage area, although no direct unconformity was observed, the basal conglomerate of the Benbatu Formation can be considered as a molassic deposition, with abundant volcanic boulders and pebbles (Fig. 5a). Meanwhile, the unconformity between the Late Carboniferous basal conglomerate and ophiolite was identified in the Aerbaolage area (Fig. 10b; Zhang et al., 2012). In the West-Ujimqin area, the basal conglomerate of Benbatu Formation unconformably covered the Precambrian Xilinhot metamorphic complex (Bao et al., 2006) and showed a molassic-like feature. However, for the Aohanqi area, the first Early Carboniferous deposits were carbonates whereas basal sediments are unclear as no pre-Carboniferous sediment was identified.

5.1.2 First stage of carbonate platform deposits

After the fining upward molassic deposition, the entire region came into a carbonate platform environment, represented by the Benbatu Formation limestone, which is characterized by the abundant shallow marine fossils (e.g. fusulinids, corals, and brachiopods) as shown in Fig. 10. The Benbatu Formation from the Sunidzuoqi, Ondor Sum, Aerbaolage, and West-Ujimqin areas can be correlated by fusulinid combinations. The *Profusulinella-Pseudostaffella* and *Fusulina-Fusulinella* zones characterize the lower and upper parts of the Benbatu Formation (IMBGMR, 1991; Li et al., 1996). Meanwhile, the Benbatu Formation can also be identified from the Siziwangqi and Alukerqin areas, which are located on both sides of the Southern Orogen (Fig. 1b). This is an indication that transgression occurred over the entirety of

central Inner Mongolia. Furthermore, a direct unconformity between the Late Carboniferous limestone and ophiolitic mélange was identified in the Ondor Sum area (Fig. 10c), indicating a transgressive overlap. During this stage, the whole area became an extensive inland sea, producing widespread carbonate deposits with similar shallow marine fossils.

5.1.3 Terrigenous deposits and local volcanism within the carbonate platform

After the Benbatu Formation carbonate deposition, terrigenous clastic sediments dominated this region with local volcanic occurrence (Fig. 10). In the Aerbaolage and Ondor Sum areas, thick-bedded coarse sandstone with large inclined beddings and cross beddings (Figs. 4d and 5g) is situated at the bottom of the Amushan Formation (Fig. 10). Furthermore, the high proportion of lithic and feldspar fragments, combined with conglomerate interlayers, indicate their low maturity, which may have been deposited in an inland sea close to the provenance. In the West-Ujimqin area, limestone pebbles within the basal conglomerate of the Amushan Formation indicate erosion of an underlying carbonate deposition. In the Sunidzuoqi-Sunidyouqi area, the Chagannur volcanic rocks are situated above the Benbatu Formation limestone (Fig. 10). The geochemical features of the basalt and rhyolite indicate an extensional setting (Tang et al., 2011). During this stage, the regional tectonics caused uplift and erosion of the underlying strata, producing clastic deposits in the nearby basins.

5.1.4 Second stage of carbonate platform deposits

Represented by the Amushan Formation limestone, a new stage of carbonate deposits overly the terrigenous sediments (Fig. 10). Like the Benbatu Formation, the

Amushan Formation can also be correlated by fusulinid fossils (e.g., *Triticites* and *Pseudoschwagerina*) throughout the entire area (IMBGMR, 1991; Li et al., 1996; Shen et al., 2006). The distribution of the Amushan Formation carbonate deposits is more widespread than that of the Benbatu Formation, indicating the expansion of the inland sea.

5.1.5 Post-carbonate terrigenous clastic deposition

Diverse depositional patterns occurred in central Inner Mongolia (Fig. 10) after deposition of the Amushan Formation carbonate. A subaerial environment followed the Amushan limestone without deposition to the south of Sunidzuoqi until the Middle-Late Permian terrestrial conglomerate (Xu and Chen, 1997). In Ondor Sum, Aerbaolage and West Ujimqin areas, shallow marine or littoral facies clastic deposits overly the Amushan limestone, and in turn were covered by the Early Permian shallow marine facies deposits (Bao et al., 2006; Gong et al., 2013). In the Aohanqi area, the Upper Carboniferous carbonate-clastic sediments were followed by the Upper Carboniferous Jiujuzi Formation terrestrial facies deposits, with Cathaysian flora and coal seams therein (IMBGMR, 1991; Figs. 10 and 7h).

5.2 Provenance interpretation and basement indication

Detrital zircon age spectra of the five sandstone samples from the Carboniferous rocks are dominated by Phanerozoic grains that exhibit two main age clusters with peaks at 400-440 Ma and 310 Ma, and subordinate peaks at 340 Ma (Fig. 9). The Early Paleozoic peak at 400-440 Ma was identified from samples near the northern

and southern suture zones, in Sunidzuoqi, Ondor Sum, and West-Ujimqin (Fig. 1b), where the Early Paleozoic arc magmatic rocks are widespread (Jian et al., 2008; Xu et al., 2013; Zhang et al., 2013). This peak can also be traced from detrital zircon results of the Early Paleozoic sediments in AXXB and SHB (Fig. 11). The 310 Ma age peak was identified from the West-Ujimqin and Aerbaolag areas, where the Late Carboniferous magmatic rocks were well exposed (Bao et al., 2007; Liu et al., 2009; Xue et al., 2010), indicating that the local magmatic rocks were the main provenance for these zircons. Furthermore, the age peak at 384 Ma is only evidenced by the sample from Aohanqi, where the same age peak was displayed from the Devonian strata (Cheng et al., 2014). This unique age cluster may be related to the Devonian syenitic complexes and mafic intrusions at the northern margin of the NCC (Luo et al., 2001; Jiang, 2005; Zhang et al., 2010; Zhang and Zhai, 2010).

Precambrian zircon grains can be traced from four samples, but a rigorous statistical comparison is impossible because of the small number of grains (Fig. 9). However, the predominant Meso- to Neo-proterozoic grains are most likely supplied from the underlying AXXB and SHB, where such a Meso- to Neo-proterozoic basement is well documented (Fig. 11; Zhang et al., 2012; Xu et al., 2013; Wang et al., 2013; Zhao et al., 2014).

In summary, the detrital zircon dating results indicate that the provenances for these Late Carboniferous strata were mainly local magmatic rocks with subordinate input of basement clastics, indicating local erosion and proximal provenances. This kind of detrital zircon distribution pattern indicates that the Carboniferous strata were

deposited above the Precambrian basement of these three blocks and two Early Paleozoic orogenic belts. Therefore, the Carboniferous strata were most likely deposited in an inland sea above the welded block, but not in a wide ocean.

5.3 Tectonic implication

The sedimentological analyses and detrital zircon dating of the Carboniferous strata in central Inner Mongolia display the same depositional setting and similar provenance, indicating that they were deposited in the same geological setting. The sedimentological analyses document that most of the Carboniferous strata overlie the Neoproterozoic basement, Early Paleozoic magmatic arc, accretionary complex, and Devonian strata. This conclusion is supported by our detrital zircon results (Figs. 9 and 11). This unconformity represents a regional transgression during the Late Carboniferous after the Devonian-Early Carboniferous sedimentary hiatus in most regions of central Inner Mongolia (Fig. 12; IMBGMR, 1991; Tang, 1990; Shao et al., 1991).

The subduction of PAO produced two arc magmatic belts along two subduction zones of opposite polarities, named the Bainaimiao Arc at the northern margin of NCC and the Baolidao Arc at the southern margin of AXXB (Fig. 12a; Jian et al., 2008; Xu et al., 2013). Both arc activities started from ca. 500 Ma, and ceased at 420-410 Ma (Jian et al., 2008; Shi et al., 2005; Zhang et al., 2013). The magmatism was accompanied by blueschist facies metamorphism (Xu et al., 2001; De Jong et al., 2006). The final continental collision was postdated by Late Silurian-Early Devonian

molassic deposition along the Southern Orogen (Fig. 12a; Tang, 1990; Zhang et al., 2010; Shi et al., 2013), and Late Devonian molassic deposition along the Northern Orogen (Fig. 12a; Xu et al., 2013). NCC, SHB, and AXXB were welded into a unified continent after two collisions (Xu et al., 2013), which is supported by recent paleomagnetic studies (Zhao et al., 2013). Except for the molassic deposition along the two orogenic belts, most parts of the central Inner Mongolia came into a subaerial environment, without Devonian-Early Carboniferous deposits (Fig. 12a; Tang, 1990; Shao et al., 1991).

During the Late Carboniferous, abundant bimodal volcanic rocks and granite emplaced, forming a huge extensional related magmatic belt in the areas of southern Mongolia and northern Inner Mongolia (Fig. 12b; Shi et al., 2003; Bao et al., 2007; Xue et al., 2010; Yarmolyuk et al., 2008; Cheng et al., 2012; Xu et al., 2012; Liang et al., 2013). Nevertheless, geochemical studies of the Late Carboniferous granitoids from Sunidzuoqi and West-Ujimqin display calc-alkaline affinities (Chen et al., 2000; Liu et al., 2009; 2013). The Late Carboniferous magmatic intrusions from Chengde area at the northern margin of NCC also display arc-like geochemistry affinities (S.H. Zhang et al., 2007; 2009a). These results were considered as evidences for the existence of magmatic arcs and oceanic subduction in central Inner Mongolia during the Late Carboniferous (Chen et al., 2000; S.H. Zhang et al., 2007; 2009a; Liu et al., 2013). However, the Late Carboniferous granitoids in West-Ujimqin were also interpreted as extension-related (Bao et al., 2007; Xue et al., 2010). The Chagannur bimodal volcanic rocks in Sunidzuoqi-Sunidyouqi were also described as forming in

post-collisional extensional setting (Tang et al., 2011). X.H. Zhang et al. (2012) reported the Late Carboniferous appinitic intrusions in Hohhot area, which were interpreted to be formed within a post-subduction transtensional regime. Moreover, he also considered that the Late Carboniferous magmatic intrusions S.H. Zhang et al. (2007; 2009a) reported in Chengde area are also belong to appinitic magmatic rocks, which should emplace in the same transtensional setting. Furthermore, these Late Carboniferous magmatic rocks can be found on both sides of the suture zone, which cannot be explained by an arc model. In addition, the arc interpretation is contradictory with our sedimentary analyses, as the Late Carboniferous deposits on both sides of this assumed Late Carboniferous arc are comparable, indicating the same sedimentary environment (Figs. 1b and 12b; IMBGMR, 1991; Shao et al., 1991). Meanwhile, the basal conglomerate of the Late Carboniferous strata uncomformably overlies the underlying Precambrian basement, ophiolitic mélange, Early Paleozoic magmatic arc, and Late Carboniferous magmatic intrusions, indicating an extensive transgression on a single continent. Hence, the Late Carboniferous magmatic rocks may be emplaced in a local extensional or transtensional trough (Fig. 12b; Bao et al., 2007; Tang et al., 2011).

Furthermore, during the Late Carboniferous, the northern Inner Mongolia (from Erenhot to East-Ujimqin) was dominated by terrestrial facies deposits (Fig. 12b), represented by the Baoligaomiao Formation, from which abundant Angara flora were identified (IMBGMR, 1991). This terrestrial deposit belt indicates the intracontinental environment of AXXB during the Late Carboniferous, which can be treated as the

northern margin of the inland sea (Fig. 12b; Bao et al., 2006).

5.4 Paleontological and paleomagnetic constraints

Our sedimentological analyses and depositional setting interpretations are consistent with both the paleontological (Zhou et al., 2010; Xin et al., 2011) and the paleomagnetic data in this region (Pruner, 1987; Xu et al., 1997; Chen et al., 1997; Li et al., 2012; Zhao et al., 2013).

In recent paleontological studies, typical Cathaysia flora fossils were identified from the Baoligaomiao Formation in East-Ujimqin, mixed with Angara flora (Xin et al., 2011). Furthermore, Cathaysia flora fossils were also identified from the Late-Middle Permian strata in East-Ujimqin (Zhou et al., 2010). Recently identified Late Carboniferous-Middle Permian mixture of Cathaysia and Angara flora in the northern part of Inner Mongolia indicate that the PAO closed at least before the Late Carboniferous. These new discoveries improved the traditional paleontological division, which considered the mixture of Cathaysia and Angara flora did not occur until the Late Permian along the Solonker (Huang, 1980; Deng et al., 2009; Shi, 2006). This pre-Late Carboniferous closure of PAO was also suggested by Dobretsov et al. (1995; 2003) and then confirmed by Safonova et al. (2009) and Donskaya et al. (2013).

Although paleomagnetic results indicate a long distance from the NCC and SIB during the Carboniferous, the intervening microblocks were located nearby the NCC since at least the Late Carboniferous (Pruner, 1987; Xu et al., 1997; Chen et al., 1997; Li et al., 2012). Xu et al. (1997) carried out paleomagnetic studies on the

Carboniferous-Permian strata from the Chita area (Amur region of Russia), and got a similar paleolatitude of the Amur block with that of NCC. From paleomagnetic studies of the Carboniferous-Permian strata from central Mongolia, Pruner (1987) considered that central Mongolia was a part of the NCC ever since the Early Permian. For the Chinese part, paleomagnetic studies were performed on the Upper Carboniferous strata in East-Ujimqin and Sunidzuoqi areas, northern Inner Mongolia, both of which gave similar paleolatitudes with NCC and placed the northern Inner Mongolia at the northern margin of NCC during the Late Carboniferous (Chen et al., 1997; Li et al., 2012). Recently, paleomagnetic studies were carried out on the Devonian-Permian strata of Hunshandake Block, showing that this block was located at the northern margin of NCC since the Late Devonian (Zhao et al., 2013). These blocks were accreted to the northern margin of NCC, and formed a large continental block before the Late Devonian (Zhao et al., 2013; Xu et al., 2013).

Conclusions

Combining our new sedimentological analyses and detrital zircon dating with previous tectonic, geochemical, geochronological, paleontological and paleomagnetic studies, we can draw the following conclusions.

(1) Widespread Late Carboniferous strata in central Inner Mongolia were dominated by shallow marine clastic-carbonate deposits with basal conglomerate above the Precambrian basement and Early Paleozoic orogens. These rocks represent a Late Carboniferous inland sea in central Inner Mongolia.

(2) Five sedimentary stages have been distinguished to depict the Carboniferous deposition. From bottom to top, they are i) basal molassic deposits, ii) first carbonate platform deposits, iii) terrigenous deposits with coeval intra-plate volcanism, iv) second carbonate platform deposits, and v) post-carbonate terrigenous deposits. These five stages represent an extensive transgression of the inland seas in central Inner Mongolia during the Late Carboniferous.

(3) The detrital zircon geochronology indicates that the provenances for these Late Carboniferous materials were mainly local magmatic rocks: erosion of the Early Paleozoic arc magmatic rocks and Carboniferous intrusions, with a subordinate input from the Precambrian basement.

(4) The sedimentary facies analyses, detrital zircon provenance, fossil assemblage similarities and paleomagnetic reconstructions indicate that an inland sea environment was the main paleogeographic feature for central Inner Mongolia during the Late Carboniferous. The Late Carboniferous inland sea strata were deposited on a continental crust, which was already welded by the Early Paleozoic collisions between NCC and the northern Songliao-Hunshandake, and the Airgin Sum-Xilinhot-Xing'an blocks.

Acknowledgments

We thank Li Ruibiao and Fang Junqin for their support in the field. This work has been funded by the National Key Basic Research Program of China (2013CB429806), the National Science Foundation of China (40872145 and 41121062). This is a

contribution to IGCP#592 “continental construction in Central Asia”.

References

Andersen, T. 2002. Correction of common lead in U-Pb analyses that do not report ^{204}Pb, Chemical Geology, 192, 59–79.

Badarch, G., Cunningham, W. D., Windley, B. F. 2002. A new terrane subdivision for Mongolia: implications for the Phanerozoic crustal growth of Central Asia. Journal of Asian Earth Sciences 21, 87–110.

Bao, Q.Z., Zhang, C.J., Wu, Z.L., Wang, H., Li, W., Sang, J.H., Liu, Y.S., 2007. SHRIMP U–Pb zircon geochronology of a carboniferous quartz diorite in Baiyingaole area, Inner Mongolia and its implications. Journal of Jilin University (Earth Science Edition) 37, 15–23 (in Chinese with English abstract).

Bao, Q.Z., Zhang, C.J., Wu, Z.L., Wang, H., Li, W., Su, Y.Z., Sang, J.H., Liu, Y.S., 2006. Carboniferous-Permian marine lithostratigraphy and sequence stratigraphy in Xi Ujimqin Qi, southeastern Inner Mongolia, China. Geological Bulletin of China 25(5), 572-579 (in Chinese with English abstract).

Burchette, T.P., and Wright, V.P., 1992. Carbonate ramp depositional systems. Sedimentary Geology 79, 3-57.

Chen, B., Jahn, B.M., Tian, W. 2009. Evolution of the Solonker suture zone: constraints from zircon U-Pb ages, Hf isotopic ratios and whole-rock Nd-Sr isotope compositions of subduction- and collision-related magmas and forearc

sediments. Journal of Asian Earth Sciences 34, 245–257.

Chen, B., Jahn, B.M., Wilde, S., Xu, B. 2000. Two contrasting Paleozoic magmatic belts in northern Inner Mongolia, China: petrogenesis and tectonic implications. Tectonophysics 328, 157–182.

Chen, C., Zhang, Z.C., Guo, Z.J., 2012. Geochronology, geochemistry, and its geological significance of the Permian Mandula mafic rocks in Damaoqi, Inner Mongolia. Science China Earth Science 55, 39–52.

Chen, H., Dobson, J.P., Heller, F., Hao, J., 1997. Preliminary paleomagneticre sultsf rom the Upper Carboniferous of Uliastai Block, Inner Mongolia, China. Geophysical Research Letters 24, 2833-2836.

Cheng, S.D., Fang, J.Q., Zhao, P., Xu, B., Bao, Q.Z., Zhou, Y.H., 2014. The Middle-Late Devonian closure of the Paleo-Asian Ocean in eastern Inner Mongolia: constraint from the detrital zircon dating results. Acta Petrologica Sinica, in press.

Cheng, Y., Teng, X., Xin, H., Yang, J., Ji, S., Zhang, Y., Li, Y., 2012. SHRIMP zircon U-Pb dating of granites in Mahonondor area, East Ujimqin Banner, Inner Mongolia. Acta Petrologica et Mineralogica 31(3), 323-334 (in Chinese with English abstract).

Choulet, F., Faure, M., Cluzel, D., Chen, Y., Lin, W., Wang, B., 2012. From oblique accretion to transpression in the evolution of the Altaid collage: New insights from West Junggar, northwestern China. Gondwana Research 21, 530-547.

Choulet, F., Faure, M., Cluzel, D., Chen, Y., Lin, W., Wang, B., Jahn, B.M., 2013.

Architecture and evolution of accretionary orogens in the altaids collage: the Earth Paleozoic west Junggar (NW China). American Journal of Science 312, 1098-1145.

Coniglio, M., Dix, G.R., 1992. Carbonate slopes. In: Walker, R.G., James, N.P. (Eds.), Facies Models: Response to Sea Level Change. Geological Association of Canada, St. John's, 349–373.

De Jong, K., Xiao, W.J., Windley, B.F., Masago, H., Lo, C.H., 2006. Ordovician $^{40}Ar/^{39}Ar$ phengite ages from the blueschist-facies Ondor Sum subduction–accretion complex (Inner Mongolia) and implications for the Early Paleozoic history of continental blocks in China and adjacent areas. American Journal of Science 306, 799–845.

Deng, S., Wan, C., Yang, J., 2009. Discovery of a Late Permian Angara–Cathaysia mixed flora from Acheng of Heilongjiang, China, with discussions on the closure of the Paleoasian Ocean. Science China Earth Science 52, 1746–1755.

Didenko, A.N., Mossakovskiy, A.A., Pecherskiy, D.M., Ruzhentsev, S.G., Samygin, S.G., and Kheraskova, T.N., 1994, Geodynamics of Paleozoic oceans of Central Asia. Russian Geology and Geophysics 35, 48-62.Dobretsov, N.L., Berzin, N.A., Buslov, M.M., 1995. Opening and tectonic evolution of the Paleo-Asian Ocean. Internal Geology Review 37, 335-360.

Dobretsov, N.L., Buslov, M.M., and Vernikovsky, V.A., 2003, Neoproterosoic to Early Ordovocian evolution of the Paleo-Asian Ocean: implications to the break-up of Rodinia. Gondwana Research 6, 143-159.

Donskaya T.V., Gladkochub D.P., Mazukabzov A.M., and Ivanov A.V., 2013. Late Paleozoic - Mesozoic subduction-related magmatism at the southern margin of the Siberian continent and the 150 million-year history of the Mongol-Okhotsk Ocean: Journal of Asian Earth Sciences 62 79-97.

Ge, M.C., Zhou, W.X., Yu, Y., Sun, J.J., Bao, J.Q., Wang, S.H., 2011. Dissolution and supracrustal rocks dating of Xilin Gol Complex, Inner Mongolia, China. Earth Science Frontiers 18(5), 182-195 (in Chinese with English abstract).

Gong, F.H., Huang, X., Chen, S.W., Zheng, Y.J., Zhang, J., Su, F., 2013. Organic geochemical characteristics of source rocks in Shoushangou Formation, Xi Ujimqin Banner of Inner Mongolia. Geological Bulletin of China 32(8), 1322-1328 (in Chinese with English abstract).

Graham, S.A., Hendrix, M.S., Johnson, C.L., Badamgarav, D., Badarch, G., Amory, J., Porte, M., Barsbold, R., Webb, L.E., Hacker, B.R., 2001. Sedimentary record and tectonic implications of Mesozoic rifting in southern Mongolia. Geological Society of America Bulletin 113, 1560-1579.

Han, B. F., Wang, S. G., Jahn, B. M., Hong, D. W., Kagami, H. and Sun, Y. L., 1997. Depleted-mantle magma source for the Ulungur River A-type granites from north Xinjiang, China: geochemistry and Nd-Sr isotopic evidence, and implication for Phanerozoic crustal growth. Chemical Geology 138, 135-159.

Han, B.F., He, G.Q., Wang, X.C., Guo, Z.J., 2011. Late Carboniferous collision between the Tarim and Kazakhstan–Yili terranes in the western segment of the South Tian Shan Orogen, Central Asia, and implications for the Northern

Xinjiang, western China. Earth-Science Review 109, 74-93.

Hendrix, M.S., Graham, S.A., Amory, J.Y., Badarch, G., 1996. Noyon Uul syncline, southern Mongolia: Lower Mesozoic sedimentary record of the tec1tonic amalgamation of central Asia. Geological Society of America Bulletin 108, 1256-1274.

Hong, D., Huang, H., Xiao, Y., Xu, H., Jin, M., 1994. The Permian alkaline granites in central Inner Mongolia and their geodynamic significance. Acta Geologica Sinica 69(3), 219-230 (in Chinese with English abstract).

Huang, B.H., 1980. Permo-Carboniferous flora of Tianshan–Xingan Fold-belt. China Science Bulletin 11, 933–936.

IMBGMR (Inner Mongolian Bureau of Geology and Mineral Resources), 1991. Regional geology of Inner Mongolian Autonomous Region. Geological Publishing House, Beijing (in Chinese with English abstract).

IMBGR, 1976. Report of geological map of China, Xianghuangqi sheet, scale 1:200000.

IMBGR, 2007. Report of geological map of China, Dongwuzhumuqinqi sheet, scale 1:250000.

Jahn, B., Wu, F., Chen, B., 2000. Massive granitoid generation in Central Asia: Nd isotope evidence and implication for continental growth in the Phanerozoic. Episodes 23, 82-92.

Jahn, B.M., Capdevila, R., Liu, D., Vernon, A., Badarch, D., 2004. Sources of Phanerozoic granitoids in the transect Bayanhongor-Ulaan Baatar, Mongolia:

geochemical and Nd isotopic evidence, and implications for Phanerozoic crustal growth. Journal of Asian Earth Science 23, 629-653.

Jahn, B.M., Litvinovsky, B.A., Zanvilevich, A.N., Reichow, M., 2009. Peralkaline granitoid magmatism in the Mongolian–Transbaikalian Belt: Evolution, petrogenesis and tectonic significance. Lithos 113, 521-539.

Jian, P., Liu, D.Y., Kröner, A., Windley, B.F., Shi, Y.R., Zhang, F.Q., Shi, G.H., Miao, L.C., Zhang, W., Zhang, Q., Zhang, L.Q., Ren, J.S., 2008. Time scale of an early to mid-Paleozoic orogenic cycle of the long-lived Central Asian Orogenic Belt, Inner Mongolia of China: implications for continental growth. Lithos 101, 233–259.

Jian, P., Liu, D.Y., Kröner, A., Windley, B.F., Shi, Y.R., Zhang, W., Zhang, F.Q., Miao, L.C., Zhang, L.Q., Tomurhuu, D., 2010. Evolution of a Permian intraoceanic arc–trench system in the Solonker suture zone, Central Asian Orogenic Belt, China and Mongolia. Lithos 118, 169-190.

Jiang, G., Gao, D., Zhang, W., Li, S., Xu, Y., Luo, F., 1995a. Patterns of sedimentary associations and evolution of sequence of Zhesi Formation in Sonid zuoqi, Inner Mongolia. Geoscience 9(2), 162-169 (in Chinese with English abstract).

Jiang, G., Zhang, W., Xiao, R., Luo, Z., Li, S., Gao, D., 1995b. Subdivision and correlation of Permian strata in Sonid zuoqi area, Inner Mongolia. Geoscience 9(2) 149-161 (in Chinese with English abstract).

Jiang, N., 2005. Petrology and geochemistry of the Shuiquangou syenitic complex, northern margin of the North China Craton. Journal of the Geological Society,

London 162, 203-215.

Johnson, C.L., 2004. Polyphase evolution of the East Gobi basin: sedimentary and structural records of Mesozoic-Cenozoic intraplate deformation in Mongolia. Basin Research 16, 79-99.

Khain, E.V., Bibikova, E.V., Kroner, A., Zhuravlev, D.Z., Sklyarov, E.V., Fedotova, A.A., Kravchenko-Berezhnoy, I.R., 2002. The most ancient ophiolites of the Central Asian fold belt: U–Pb and Pb–Pb zircon ages for the Dunzhugur complex, Eastern Sayan, Siberia, and geodynamic implications. Earth and Planetary Science Letters, 199, 311–325.

Kröner, A., Kovach, V., Belousova, E., Hegner, E., Armstong, R., Dolgopolova, A., Seltmann, R., Alexeiev, D.V., Hoffmann, J.E., Wong, J., Sun, M., Cai, K., Wang, T., Tong, Y., Wilde, S.A., Degtyarev, K.E., Rytsk, E., 2014. Reassessment of continental growth during the accretionary history of the Central Asian Orogenic Belt. Gondwana Research 25, 103-125.

Li, J.Y., 2006. Permian geodynamic setting of Northeast China and adjacent regions: closure of the Paleo-Asian Ocean and subduction of the Paleo-Pacific Plate. Journal of Asian Earth Sciences 26, 207-224.

Li, P., Zhang, S., Gao, R., Li, H., Zhao, Q., Li, Q., Guan, Y., 2012. New Upper Carboniferous-Lower Permian Paleomagnetic Results from the Central Inner Mongolia and Their Geological Implications. Journal of Jilin University (Earth Science Edition) 42, 423-440 (in Chinese with English abstract).

Li, W.G., Li, Q.F., Jiang, W.D., 1996. Lithostratigraphy of Inner Mongolia

Autonomous Region. Chinese University of Geoscience Press, Beijing. pp. 1-344 (in Chinese).

Li, Y.L., Zhou, H.W., Brouwer, F.M., Wijbrans, J.R., Zhong, Z.Q., Liu H.F., 2010. Tectonic significance of the Xilin Gol Complex, Inner Mongolia, China: Petrological, geochemical and U–Pb zircon age constraints. Journal of Asian Earth Sciences 42, 1018-1029.

Liang, Y., Yu, C., Shen, G., Sun, Q., Li, J., Yang, Y., She, H., Zhang, B., Tan, G., 2013. Geochemical characteristics of granites in the Suonaga Pb-Zn-Ag deposit of Dong Wjimqin Banner, Inner Mongolia, and their tectonic and ore-forming implications. Geology in China 40, 767-779 (in Chinese with English abstract).

Liang, Y., Yu, C., Shen, G., Sun, Q., Li, J., Yang, Y., She, H., Zhang, B., Tan, G., 2013. Geochemical characteristics of granites in the Suonaga Pb-Zn-Ag deposit of Dong Ujimqin Banner, Inner Mongolia, and their tectonic and ore-forming implications. Geology in China 40(3), 767-779 (in Chinese with English abstract).

Liu, J., Chi, X., Zhang, X., Ma, Z., Zhao, Z., Wang, T., Hu, Z., Zhao, X., 2009. Geochemical characteristic of Carboniferous quartz-diorite in the southern Xiwuqi area, Inner Mongolia and its tectonic significance. Acta Geologica Sinica 83, 365-376 (in Chinese with English abstract).

Liu, J., Li, J., Chi, X., Qu, J., Hu, Z., Fang, F., Zhang, Z., 2013. A late-Carboniferous to early early-Permian subduction–accretion complex in Daqing pasture, southeastern Inner Mongolia: Evidence of northward subduction beneath the

Siberian paleoplate southern margin. Lithos 177, 285-296.

Ludwig, K.R., 2003. User's Manual for Isoplot 3.0: A Geochronological Toolkit for Microsoft Excel Berkeley Geochronology Center. special publication, 4, pp. 1–71.

Luo, Z., Miao, L., Guan, K., Qiu, Y., Qiu, Y.M., McNaughton, N.J., Groves, D.I., 2001. SHRIMP chronological study of Shuiquangou intrusive body in Zhangjiakou area, Hebei Province and its geochemical significance. Geochimica 30, 116–122 (in Chinese with English abstract).

Meng, Q.R., 2003. What drove late Mesozoic extension of the northern China–Mongolia tract? Tectonophysics 369, 155-174.

Miao, L., Qiu, Y., McNaughton, N., Luo, Z., Groves, D., Zhai, Y., Fan, W., Zhai, M., Guan, K., 2002. SHRIMP U–Pb zircon geochronology of granitoids from Dongping area, Hebei Province, China: constraints on tectonic evolution and geodynamic setting for gold metallogeny. Ore Geology Reviews 19, 187–204.

Mueller, J. F., Rogers, J. J. W., Jin, Y. G., Wang, H., Li, W., Chronic, J., Mueller J. F., 1991. Late Carboniferous to Permian sedimentation in Inner Mongolia, China, and tectonic relationships between north China and Siberia, Journal of Geology 99, 251–263.

Prothero, D.R. and Schwab, F., 2003. Sedimentary Geology An introduction to sedimentary rocks and stratigraphy. New York: W.H. Freeman and Company, pp.1-557.

Pruner, P., 1987. Palaeomagnetism and palaeogeography of Mongolia in the

Cretaceous, Permian and Carboniferous-preliminary data, Tectonophysics 139, 155–167, doi:10.1016/0040-1951(87)90204-6.

Safonova, I.Yu., 2009, Intraplate magmatism and oceanic plate stratigraphy of the Paleo-Asian and Paleo-Pacific Oceans from 600 to 140 Ma. Ore Geology Reviews 35, 137-154.

Safonova, I.Yu., Utsunomiya, A., Kojima, S., Nakae, S., Koizumi, K., Tomurtogoo, O., Filippov, A.N., 2009. Pacific superplume-related oceanic basalts hosted by accretionary complexes of Central Asia, Russian Far East and Japan. Gondwana Research 16, 587-608.

Safonova, I.Yu., and Santosh, M., 2014, Accretionary complexes in the Asia-Pacific region: Tracing archives of ocean plate stratigraphy and tracking mantle plumes. Gondwana Research 25, 126-158.

Safonova, I.Yu., Seltmann, R., Kröner, A., Gladkochub, D., Schulmann, K., Xiao, W.J., Kim, J.Y., Komiya, T., and Sun, M., 2011, A new concept of continental construction in the Central Asian Orogenic Belt. Episodes 34, 186-196.Sengör, A.M.C., Natal'in, B.A., Burtman, V.S., 1993. Evolution of the Altaid tectonic collage and Palaeozoic crustal growth in Eurasia. Nature 364, 299–307.

Shao, J.A., 1991. Crust Evolution in the Middle Part of the Northern Margin of Sino-Korean Plate, Peking University Press, Beijing, pp. 1-136 (in Chinese with English abstract).

Shen, S.Z., Zhang, H., Shang, Q.H., Li, W.Z., 2006. Permian stratigraphy and correlation of Northeast China: A review. Journal of Asian Earth Sciences 26,

304-326.

Shi, G.R., 2006. The marine Permian of East and Northeast Asia: an overview of biostratigraphy, palaeobiogeography and palaeogeographical implications. Journal of Asian Earth Science 26, 175–206.

Shi, G., Faure, M., Xu, B., Zhao, P., Chen, Y., 2013. Structural and kinematic analysis of the Early Paleozoic Ondor Sum-Hongqi mélange belt, eastern part of the Altaids (CAOB) in Inner Mongolia, China. Journal of Asian Earth Science 66, 123-139.

Shi, G.H., Liu, D.Y., Zhang, F.Q., Jiang, P., Miao, L.C., Shi, Y.R., Tao, H., 2003. SHRIMP U-Pb zircon geochronology and its implications on the Xilin Gol Complex, Inner Mongolia, China. Chinese Science Bulletin 48, 2742-2748.

Shi, Y.R., Liu, D.Y., Jian, P., Zhang, Q., Zhang, F.Q., Miao, L.C., Shi, G.H., Zhang, L.Q., Tao, H., 2005. Zircon SHRIMP dating of K-rich granites in Sonidzuoqi, central Inner Mongolia. Geological Bulletin of China 24(5), 424-428 (in Chinese with English abstract).

Sun, L.X., Ren, B.F., Zhao, F.Q., Gu, Y.C., Li, Y.F., Liu, H., 2013. Zircon U-Pb dating and Hf isotopic compositions of the Mesoporterozoic granitic gneiss in Xilinhot Block, Inner Mongolia. Geological Bulletin of China 32(2/3), 327-340 (in Chinese with English abstract).

Tang, K.D., 1990. Tectonic development of Paleozoic fold belts at the north margin of the Sino–Korean craton. Tectonics 9, 249-260.

Tang, K., and Yan, Z., 1993. Regional metamorphism and tectonic evolution of the

Inner Mongolian suture zone. Journal of Metamorphic Geology 11, 511-522.

Tang, W.H., Zhang, Z.Z., Li, J.F., Feng, Z.S., Chen, C., 2011. Geochemistry of the Carboniferous Volcanic Rocks of Benbatu Formation in Sonid Youqi，Inner Mongolia and Its Geological Significance. Acta Scientiarum Naturalium Universitatis Pekinensis 47(2), 321-330 (in Chinese with English abstract).

Wang, C., Wang, P., Li, W., 2004. Conodonts from the Permian Jisu Honguer (Zhesi) Formation of Inner Mongolia, China. Geobios 37, 471-480.

Wang, F., Xu, W.L., Gao, F.H., Zhang, H.H., Pei, F.P., Zhao, L., Yang, Y., 2013. Precambrian terrane within the Songnen–Zhangguangcai Range Massif, NE China: Evidence from U–Pb ages of detrital zircons from the Dongfengshan and Tadong groups. Gondwana Research, http://dx.doi.org/10.1016/j.gr.2013.06.017

Wang, T., Zheng, Y.D., Gehrels, G.E., Mu, Z.G., 2001.Geochronological evidence for existence of the south Mongolian microcontinent: a zircon U–Pbage of granitoid gneisses from the Yagan–OnchHayrhan metamorphic core complex on the Sino–Mongolian border. China Science Bulletin 46, 2005–2008.

Wilhem, C., Windley, B.F., Stampfli, G.M., 2012. The Altaids of Central Asia: A tectonic and evolutionary innovative review. Earth-Science Reviews 113, 303-341.

Windley, B.F., Alexeiev, D., Xiao, W.J., Kröner, A., Badarch, G., 2007. Tectonic models for accretion of the Central Asian Orogenic Belt. Journal of the Geological Society of London 164, 31–47.

Wu, F.Y., Zhao, G.C., Sun, D.Y., Wilde, S.A., Zhang, J.H., 2007. The Hulan Group: its

role in the evolution of the Central Asian Orogenic Belt of NE China. Journal of Asian Earth Sciences 30, 542–556.

Xiao, W., Windley, B.F., Huang, B.C., Han, C.M., Yuan, C., Chen, H.L., Sun, M., Sun, S., Li, J.L., 2009. End-Permian to mid-Triassic termination of the accretionary processes of the southern Altaids: implications for the geodynamic evolution, Phanerozoic continental growth, and metallogeny of Central Asia. International Journal of Earth Science 98, 1189–1287.

Xiao, W.J., Windley, B., Hao, J., Zhai, M.G., 2003. Accretion leading to collision and the Permian Solonker suture, Inner Mongolia, China: termination of the Central Asian Orogenic Belt. Tectonics 22, 1069–1089.

Xiao, W., Huang, B., Han, C., Sun, S., Li, J., 2010. A review of the western part of the Altaids: a key to understanding the architecture of accretionary orogens. Gondwana Research 18, 253–273.

Xiao, W., Santosh, M., 2014. The western Central Asian Orogenic Belt: A window to accretionary orogenesis and continental growth, Gondwana Research, http://dx.doi.org/10.1016/j.gr.2014.01.008

Xin, H.T., Teng, X.J., Cheng, Y.H., 2011. Stratigraphic Subdivision and Isotope Geochronology Study on the Baoligaomiao Formation in the East Ujimqin County, Inner Mongolia. Geological Survey and Research 34(1), 1-9 (in Chinese with English abstract).

Xu, B., Charvet, J., Chen, Y., Zhao, P., Shi, G.Z., 2013. Middle Paleozoic convergent orogenic belts in western Inner Mongolia (China): framework, kinematics,

geochronology and implications for tectonic evolution of the Central Asian Orogenic Belt. Gondwana Research 23, 1324-1364.

Xu, B., Charvet, J., Zhang, F.Q., 2001. Primary study on petrology and geochronology of the blueschist in Sonid Zuoqi, northern Inner Mongolia. Chinese Journal of Geology 36, 424–434 (in Chinese with English abstract).

Xu, B., Chen, B., 1997. Framework and evolution of the middle Paleozoic oroginic belt between Siberian and North China Plates in northern Inner Mongolia. Science in China (series D) 40(5), 463-469.

Xu, B., Zhao, P., Bao, Q.Z., Zhou, Y.H., Wang, Y.Y., Luo, Z.W., 2014. The pre-Mesozoic tectonic unit division of the Xing-Meng orogenic belt (XMOB). Acta Petrologica Sinica, in press.

Xu, L.Q., Ju, W.X., Liu, C., He, H.Y., Li, M.Y., 2012. Sr-Yb classification and genesis of Late Carboniferous granites in Arenshaobu area of Erenhot, Inner Mongolia. Geological Bulletin of China 31(9), 1410-1419 (in Chinese with English abstract).

Xu, X., W. Harbert, S. Dril, and V. Kravchinksy ,1997, New paleomagnetic data from the Mongol–Okhotsk collision zone, Chita region, south-central Russia: Implications for Paleozoic paleogeography of the Mongol–Okhotsk Ocean, Tectonophysics, 269, 113–129, doi:10.1016/S0040-1951(96)00140-0.

Xue, H., Guo, L., Hou, Z., Tong, Y., Pan, X., Zhou, X., 2010. SHRIMP zircon U-Pb ages of the middle Neopaleozoic unmetamorphosed magmatic rocks in the southwestern slope of the Da Hinggan Mountains, Inner Mongolia. Acta

Petrologica et Mineralogica 29(6), 811-823 (in Chinese with English abstract).

Xue, H.M., Guo, L.J., Hou, Z.Q., Zhou, X.W., Tong, Y., Pan, X.F., 2009. The Xilingele complex from the eastern patof t he Central Asian-Mongolia Orogenic Belt, China：Products of Early Variscan orogeny other than ancient block: Evidence from zircon SHRIMP U-Pb ages. Acta Petrologica Sinica 25(8), 2001-2010 (in Chinese with English abstract).

Yarmolyuk V. V., KovalenkoV. I., Sal'nikova E. B., Kozakov, I. K., Kotov, A. B., Kovach, V. P., Vladykin, N. V., and Yakovleva, S. Z., 2005. U–Pb Age of Syn- and Postmetamorphic Granitoids of South Mongolia: Evidence for the Presence of Grenvillides in the Central Asian Foldbelt. Doklady Earth Sciences 404(7), 986-990.

Yarmolyuk V. V., KovalenkoV. I., Sal'nikova E. B., Kovach, V. P., Kozlovsky, A.M., Kotov, A.B., Lebedev, V.I., 2008. Geochronology, Igneous Rocks and Formation of the Late Paleozoic South Mongolian Active Margin of the Siberian Continent. Stratigraphy and Geological Correlation 16(2),162–181.

Yu, J., Wang, F., Xu, W.L., Gao, F., Tang, J., 2013. Late Permian tectonic evolution at the southeastern margin of the Songnen–Zhangguangcai Range Massif, NE China: Constraints from geochronology and geochemistry of granitoids. Gondwana Research 24, 635-647.

Yuan, C., Sun, M., Wilde, S., Xiao, W., Xu, Y., Long, X., Zhao, G., 2010. Post-collisional plutons in the Balikun area, East Chinese Tianshan: Evolving magmatism in response to extension and slab break-off. Lithos 119, 269-288.

Zhang, S.H., Zhao, Y., Song, B., Yang, Z.Y., Hu, J.M., 2007. Carboniferous granitic plutons from the northern margin of the North China block: implications for a late Palaeozoic active continental margin. Journal of the Geological Society, London 164, 451-463.

Zhang, S. H., Zhao, Y., Song, B., Hu, J. M., Liu, S. W., Yang, Y. H., Chen, F. K., Liu, X. M., Liu, J., 2009a. Contrasting late Carboniferous and late Permian-middle Triassic intrusive suites from the northern margin of the north China craton. Geological Society of America Bulletin 121, 181-200.

Zhang, S.H., Zhao, Y., Liu, X.C., Liu, D.Y., Chen, F., Xie, L.W., Chen, H.H., 2009b. Late Paleozoic to Early Mesozoic mafic–ultramafic complexes from the northern North China Block: Constraints on the composition and evolution of the lithospheric mantle. Lithos 110, 229-246.

Zhang, W., Jian, P., Kröner, A., Shi, Y.R., 2013. Magmatic and metamorphic development of an early to mid-Paleozoic continental margin arc in the southernmost Central Asian Orogenic Belt, Inner Mongolia, China. Journal of Asian Earth Sciences 72, 63-74.

Zhang, X.H., Wilde, S.A., Zhang, H.F., Zhai, M.G., 2011. Early Permian high-K calc-alkaline volcanic rocks from NW Inner Mongolia, North China: geochemistry, origin and tectonic implications. Journal of the Geological Society, London, 168, 525-543.

Zhang, X.H., Zhai, M.G., 2010. Magmatism and its metallogenetic effects during the

Paleozoic continental crustal construction in northern North China: an overview. Acta Petrologica Sinica, 26(5), 1329-1341 (in Chinese with English abstract).

Zhang, X.H., Zhang, H.F., Jiang, N., Zhai, M., Zhang, Y., 2010. Early Devonian alkaline intrusive complex from the northern North China Craton: a petrological monitor of post-collisional tectonics. Journal of the Geological Society 167, 717-730.

Zhang, X.H., Zhang, H.F., Tang, Y.J., Wilde, S.A., Hu, Z.C., 2008. Geochemistry of Permian bimodal volcanic rocks from Central Inner Mongolia, North China: Implication for tectonic setting and Phanerozoic continental growth in Central Asian Orogenic Belt. Chemical Geology 249, 261–281.

Zhang, X.H., Gao, Y., Wang, Z., Liu, H., Ma, Y., 2012. Carboniferous appinitic intrusions from the northern North China craton: geochemistry, petrogenesis and tectonic implications. Journal of the Geological Society, London 169, 337-351.

Zhang, X.Z., Ma, Y.X., Chi, X.G., Zhang, F.X., Sun, Y.W., Guo, Y., Zeng, Z., 2012. Discussion on Phanerozoic Tectonic Evolution in Northeastern China. Journal of Jilin University (Earth Science Edition) 42(5), 1269-1285 (in Chinese with English Abstract).

Zhang, Y.P., Su, Y.Z., Li, J.C., 2010. Regional tectonics significance of the Late Silurian Xibiehe Formation in central Inner Mongolia, China. Geological Bulletin of China 29(11), 1599-1605 (in Chinese with English abstract)

Zhao, P., Chen, Y., Xu, B., Faure, M., Shi, G., Choulet, F., 2013. Did the Paleo-Asian Ocean between North China Block and Mongolia Block exist during the late

Paleozoic? First paleomagnetic evidence from central-eastern Inner Mongolia, China. Journal of Geophysical Research: Solid Earth 118, 1873-1894.

Zhao, P., Fang, J., Xu, B., Chen, Y., Faure, M., 2014. Early Paleozoic tectonic evolution of the Xing-Meng Orogenic Belt: constraints from detrital zircon geochronology of western Erguna-Xing'an Block, North China, Journal of Asian Earth Sciences, doi: http://dx.doi.org/10.1016/j.jseaes.2014.04.011

Zhou, J.B., Wilde, S.A., 2013. The crustal accretion history and tectonic evolution of the NE China segment of the Central Asian Orogenic Belt. Gondwana Research 23, 1365-1377.

Zhou, Z.G., Gu, Y.C., Liu, C.F., Yu, Y.S., Zhang, B., Tian, Z.J., He, F.B., Wang, B.R., 2010. Discovery of Early -Middle Permian cathaysian flora in Manduhubaolage area, Dong Ujimqin Qi, Inner Mongolia, China and its geological significance. Geological Bulletin of China 29(1), 21-25 (in Chinese with English abstract).

Zorin, Y.A., 1999. Geodynamics of the western part of the Mongol–Okhotsk collisional belt, Trans-Baikal region (Russia) and Mongolia. Tectonophysics 306, 33–56.

Figure and table captions

Table 1. Summary of sandstone samples for detrital zircon dating

Figure 1. (a) Location of the Altaid /Central Asian Orogenic Belt (CAOB) (compiled from Sengör et al., 1993; Windley et al., 2007). (b) Sketch geological map of

central Inner Mongolia showing the main tectonic units: three blocks (North China Craton, Songliao-Hunshandake Block, and Airgin Sum-Xilinhot-Xing'an Block) and two Early Paleozoic orogenic belts (Southern Orogen and Northern Orogen) (compiled from Jian et al., 2008; Xu et al., 2013). Carboniferous strata, highlighted in this map, were compiled from IMBGMR, (1991).

Figure 2. Comparison of stratigraphic sequences of the five locations in central Inner Mongolia, illustrating the sandstone samples used for detrital zircon dating.

Figure 3. Stratigraphic sequence and photographs of the Carboniferous strata in Sunidzuoqi (S-1 in Fig. 1b). The position of each photograph is marked beside the column. a: purple lithic sandstone; b: inclined bedding; c: wavy bedding; d: bedding-parallel mud nodules; e: inclined bedding; f: flat bedding; g: limestone with sandstone breccias; h: bioclastic limestone. The legend is used for Figure 3 to Figure 7.

Figure 4. Stratigraphic sequence and photographs of the Carboniferous strata in Ondor Sum (S-2 in Fig. 1b). The position of each photograph is marked beside the column. a: quartz-rich coarse sandstone; b: thin-layered black siltstone; c: plant fossils within black siltstone; d: large-scale cross bedding; e: sandstone interbedded with mudstone; f: massive sparite and bioclastic limestone; g: fusulinids within limestone; h: pebbly sandstone layers within limestone

sequence.

Figure 5. Stratigraphic sequence and photographs of the Carboniferous strata in Aerbaolage (S-3 in Fig. 1b). The position of each photograph is marked beside the column. a: conglomerate at the bottom of Benbatu Formation; b: corals within limestone layers; c: yellow siltstone at the top of Bentabu Formation; d: horizontal bedding; e: soft sediment deformation; f: coarse sandstone interbedded with sandstone; g: cross bedding; h: the contact between black siltstone and massive sandstone.

Figure 6. Stratigraphic sequence and photographs of the Carboniferous strata in West-Ujimqin (S-4 in Fig. 1b). The position of each photograph is marked beside the column. a: fining upward sequence at the bottom of Benbatu Formation; b: inclined bedding in coarse sandstone; c: brecciated intraclasts in limestone; d: basal conglomerate at the bottom of the Amushan Formation; e: intraclast limestone and Crinoidea therein; f: inclined bedding in sandstone; g: soft sediment deformation; h: coarse sandstone with mud breccias.

Figure 7. Stratigraphic sequence and photographs of the Carboniferous strata in Aohanqi (S-5 in Fig. 1b). The position of each photograph is marked beside the column. a: massive limestone; b: siltstone interlayer within limestone; c: corals in limestone; d: thin-bedded bioclastic limestone; e: limestone interbedded with

siltstone; f: fining upward sequence of the Jiujuzi Formation sandstone; g: plant fossils in black shale; h: burrows in black shale.

Figure 8. Cathodoluminescence (CL) images of selected detrital zircons from each sample. The circles represent U–Pb analytical sites with numbers in the circles and ages presented below.

Figure 9. U–Pb concordia and probability diagrams of zircon ages of the five sandstones in this study. The inset figures within each U-Pb concordia diagram show zircon grains with ages of 250-500 Ma.

Figure 10. Tentative correlation diagram for the five sections analyzed in this study. See Fig. 1b for locations of each section. Correlations were established by tracing similar beds in the field. Five sedimentary stages were distinguished according to different rock assemblages and sedimentary facies. a: Unconformity between Upper Devonian conglomerate and ophiolitic mélange in Sunidzuoqi (from Xu et al., 2013); b: Unconformity between Upper Carboniferous conglomerate and ophiolite in Aerbaolage (from Zhang et al., 2012); c: Unconformity between Upper Carboniferous limestone and ophiolitic mélange in Ondor Sum.

Figure 11. Comparison of probability plots for Carboniferous data from Sunidzuoqi (a)

and West-Ujimqin (b) of this study with the Early Paleozoic data from Airgin Sum-Xilinhot-Xing'an Block (AXXB) (c; Zhao et al., 2014) and Songliao-Hunshandake Block (SHB) (d; Xu et al., 2013).

Figure 12. Schematic evolutionary model between the North China Craton, Songliao-Hunshandake Block and Airgin Sum-Xilinhot-Xing'an Block (AXXB) during the Carboniferous. Detailed interpretations are given in the text.

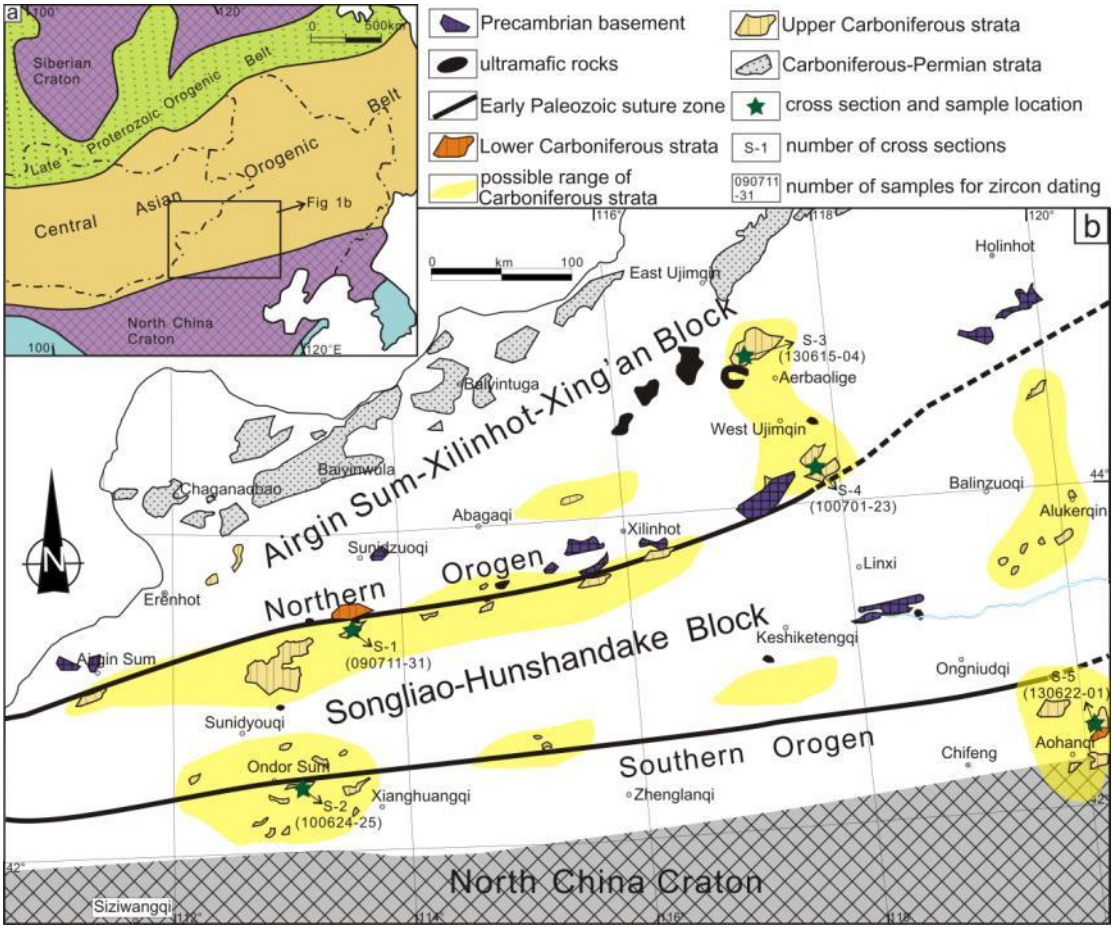

Figure 1. (a) Location of the Central Asian Orogenic Belt (CAOB, compiled from Sengör et al., 1993). (b) Sketch geological map of central Inner Mongolia showing the main tectonic units: three blocks (North China Block, Songliao-Hunshandake Block and Airgin Sum-Xilinhot-Xing'an Block) and two Early Paleozoic orogenic belts (Southern Orogen and Northern Orogen) (compiled from Jian et al., 2008; Xu et al., 2013). The Carboniferous strata, highlighted in this map, are compiled from IMBGMR, (1991). Note that they cover on the three blocks.

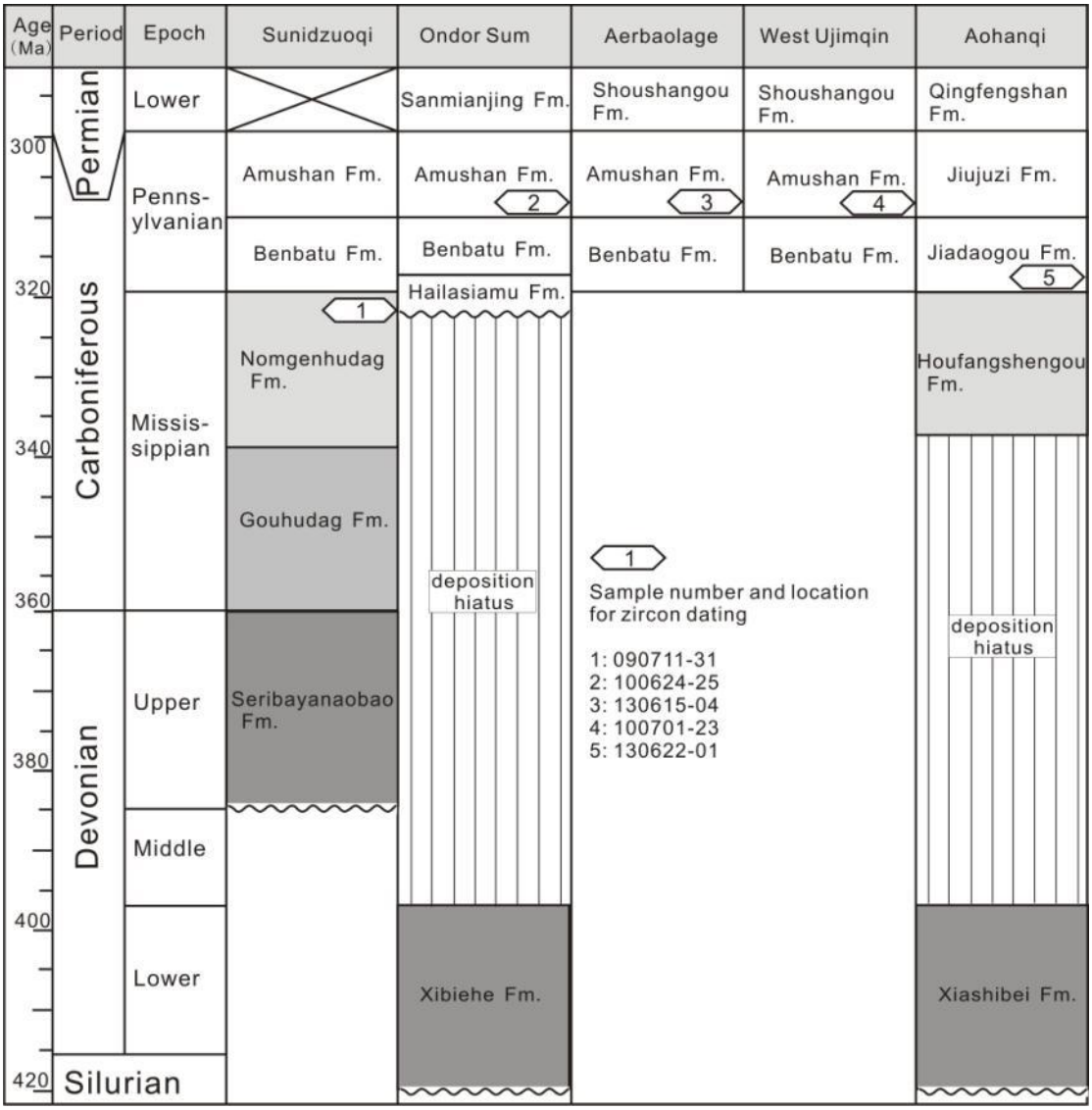

Fig. 2. Comparison of stratigraphic sequences of the five locations in central Inner Mongolia, with sandstone samples for detrital zircon dating illustrated.

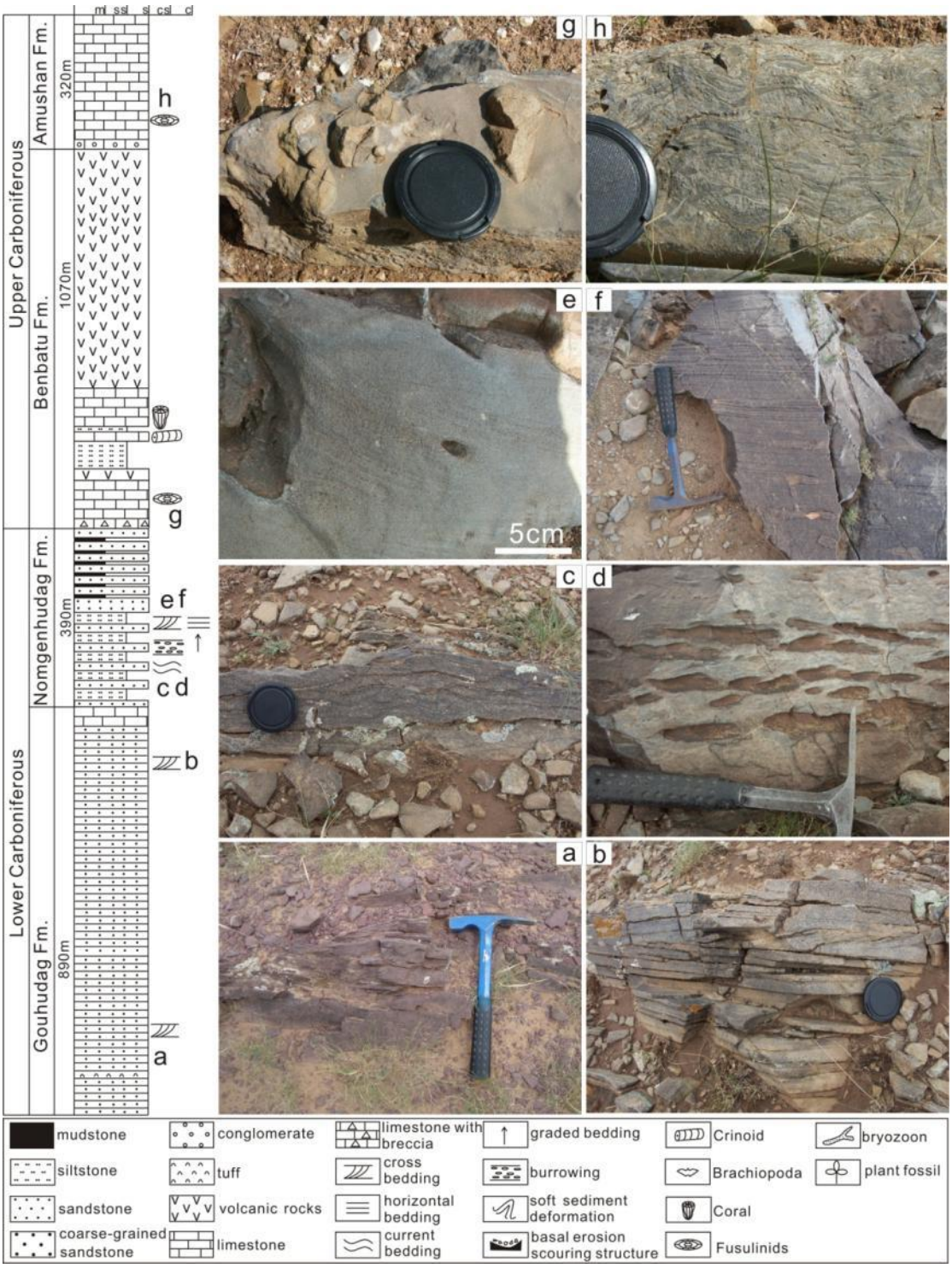

Fig. 3 Stratigraphic sequence and photographs of the Carboniferous strata in Sunidzuoqi (S-1 in Fig. 1b). The position of each photograph is marked besides the column. a: purple lithic sandstone; b: inclined bedding; c: wave bedding; d: bedding-parallel mud nodules; e: inclined bedding; f: flat bedding; g: limestone with sandstone breccias; h: bioclastic limestone. The legend is used for Figure 3 to figure 7.

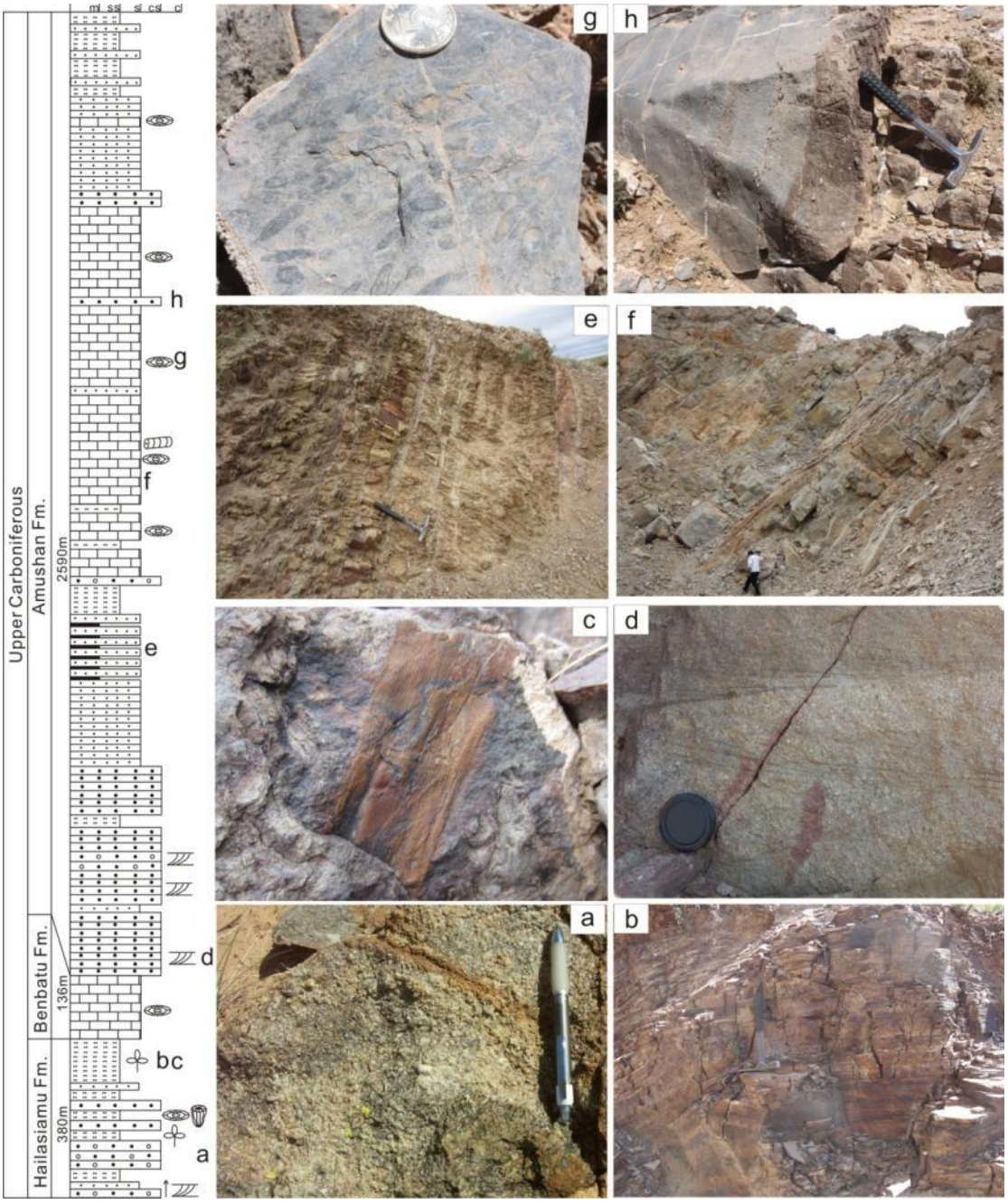

Fig. 4. Stratigraphic sequence and photographs of the Carboniferous strata in Ondor Sum (S-2 in Fig. 1b). The position of each photograph is marked besides the column. a: quartz-rich coarse sandstone; b: thin-layered black siltstone; c: plant fossils within black siltstone; d: large-scale cross bedding; e: sandstone interbedded with mudstone; f: massive sparite and bioclastic limestone; g: fusulinids within limestone; h: pebbly sandstone layers within limestone sequence.

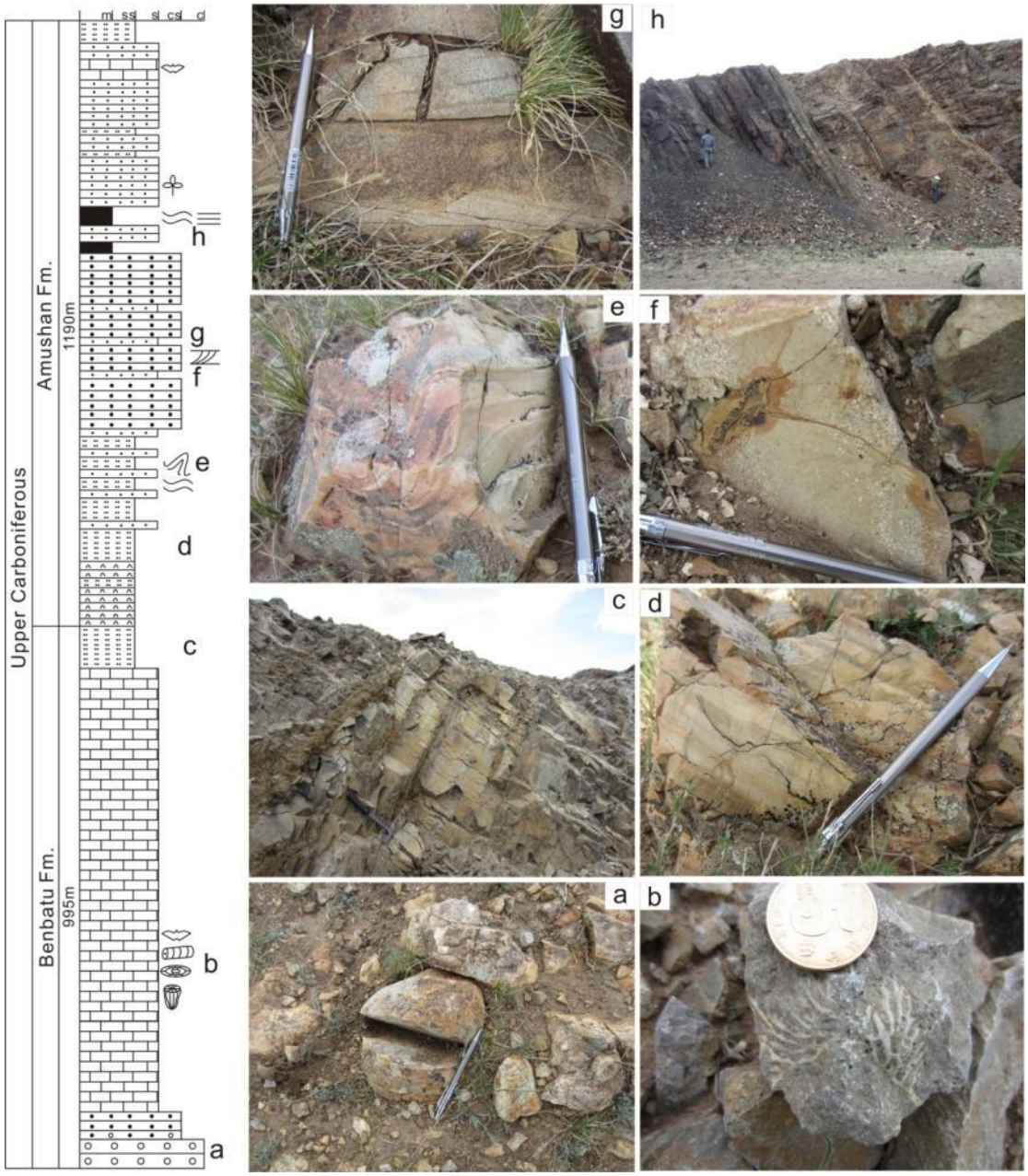

Fig. 5. Stratigraphic sequence and photographs of the Carboniferous strata in Aerbaolage (S-3 in Fig. 1b). The position of each photograph is marked besides the column. a: conglomerate at the bottom of Benbatu Formation; b: corals within limestone layers; c: yellow siltstone at the top of Bentabu Fromation; d: horizontal bedding; e: soft sediment deformation; f: coarse sandstone interbedded with sandstone; g: cross bedding; h: the contact between black siltstone and massive sandstone.

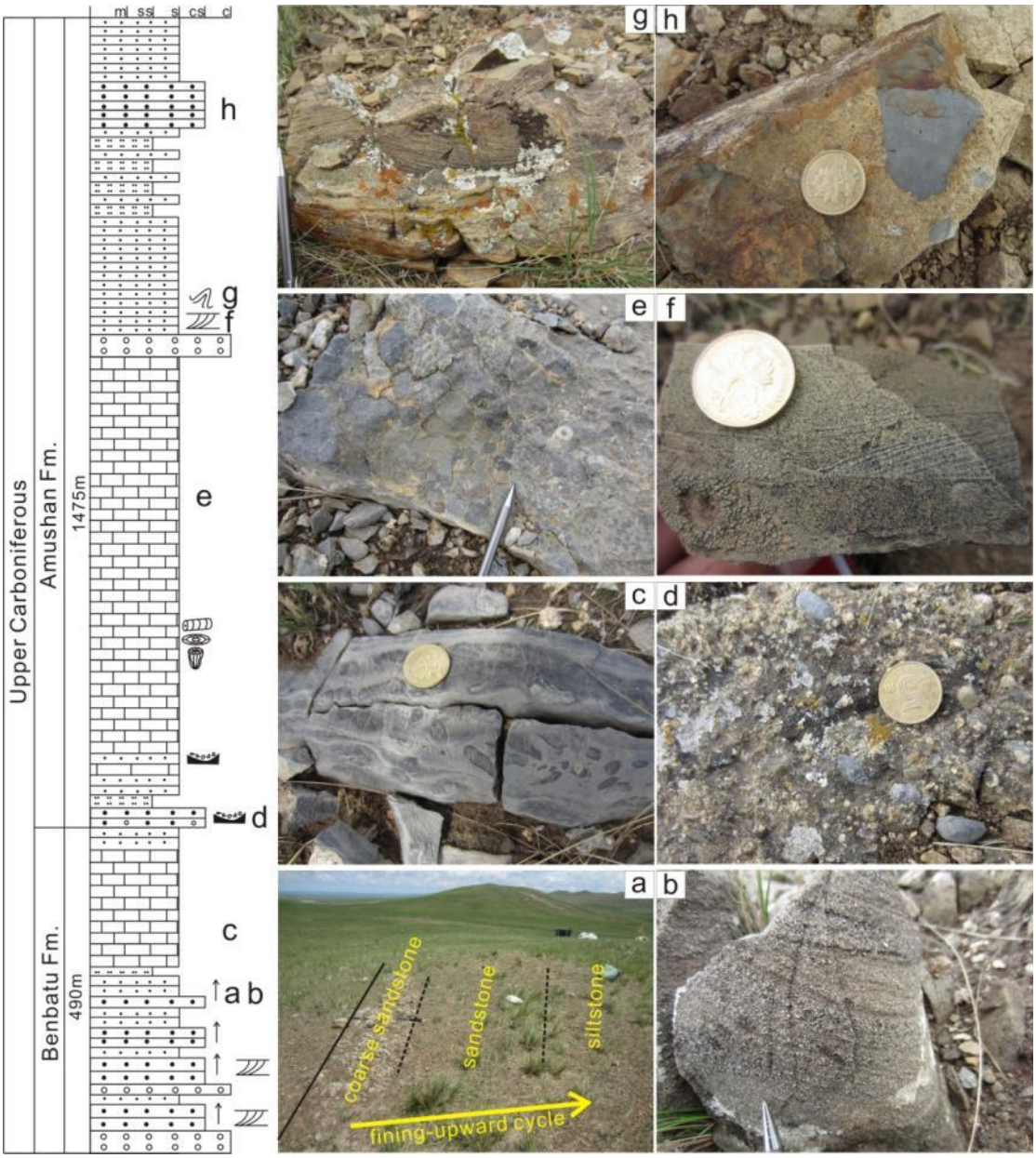

Fig. 6. Stratigraphic sequence and photographs of the Carboniferous strata in West-Ujimqin (S-4 in Fig. 1b). The position of each photograph is marked besides the column. a: fining upward sequence at the bottom of Benbatu Fromation; b: inclined bedding in coarse sandstone; c: brecciated intraclasts in limestone; d: basal conglomerate at the bottom of the Amushan Formation; e: intraclast limestone and Crinoidea therein; f: inclined bedding in sandstone; g: soft sediment deformation; h: coarse sandstone with mud breccias.

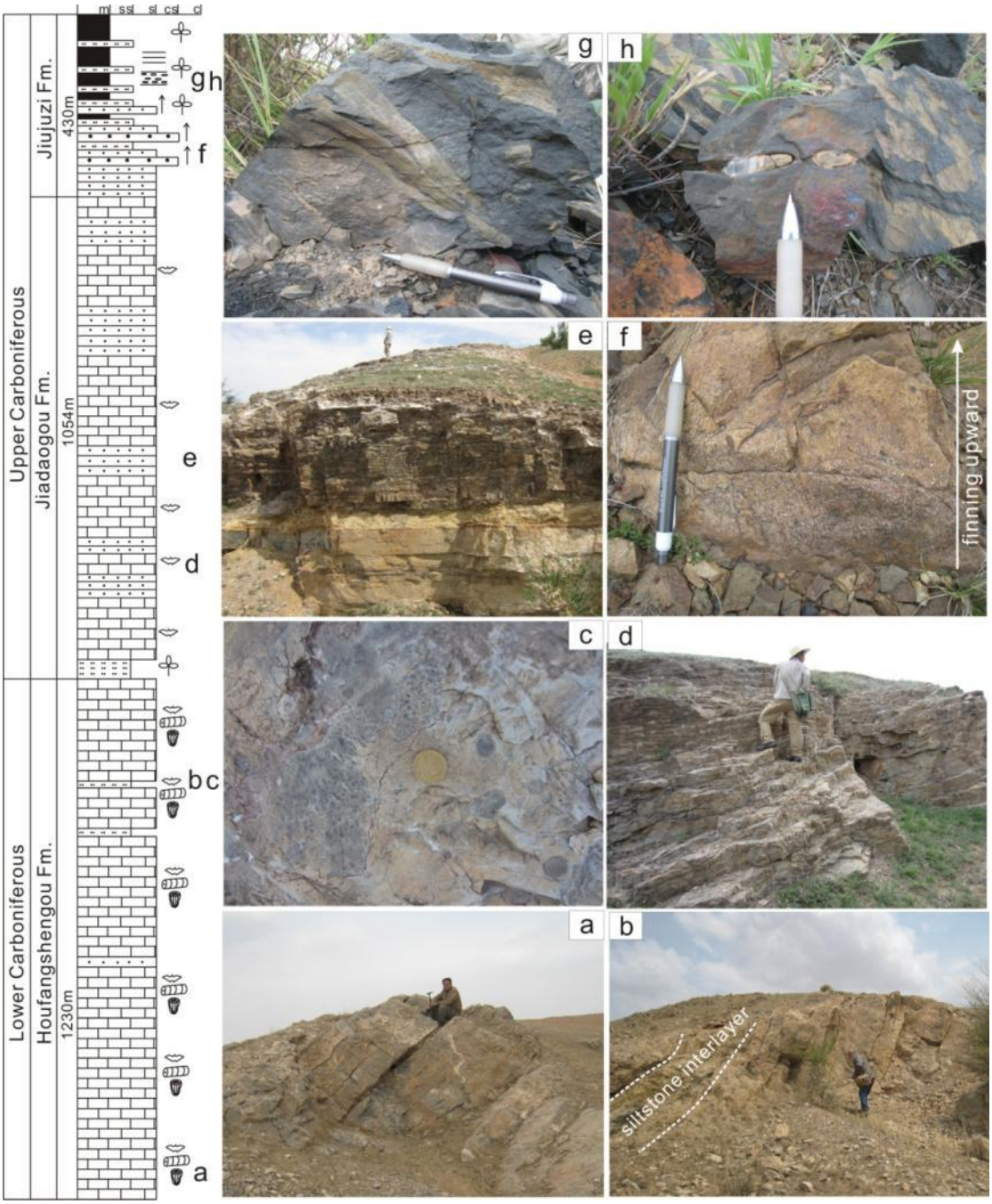

Fig. 7. Stratigraphic sequence and photographs of the Carboniferous strata in Aohanqi (S-5 in Fig. 1b). The position of each photograph is marked besides the column. a: massive limestone; b: siltstone interlayer within limestone; c: corals in limestone; d: thin-bedded bioclastic limestone; e: limestone interbedded with siltstone; f: fining upward sequence of the Jiujuzi Formation sandstone; g: plant fossils in black shale; h: burrows in black shale.

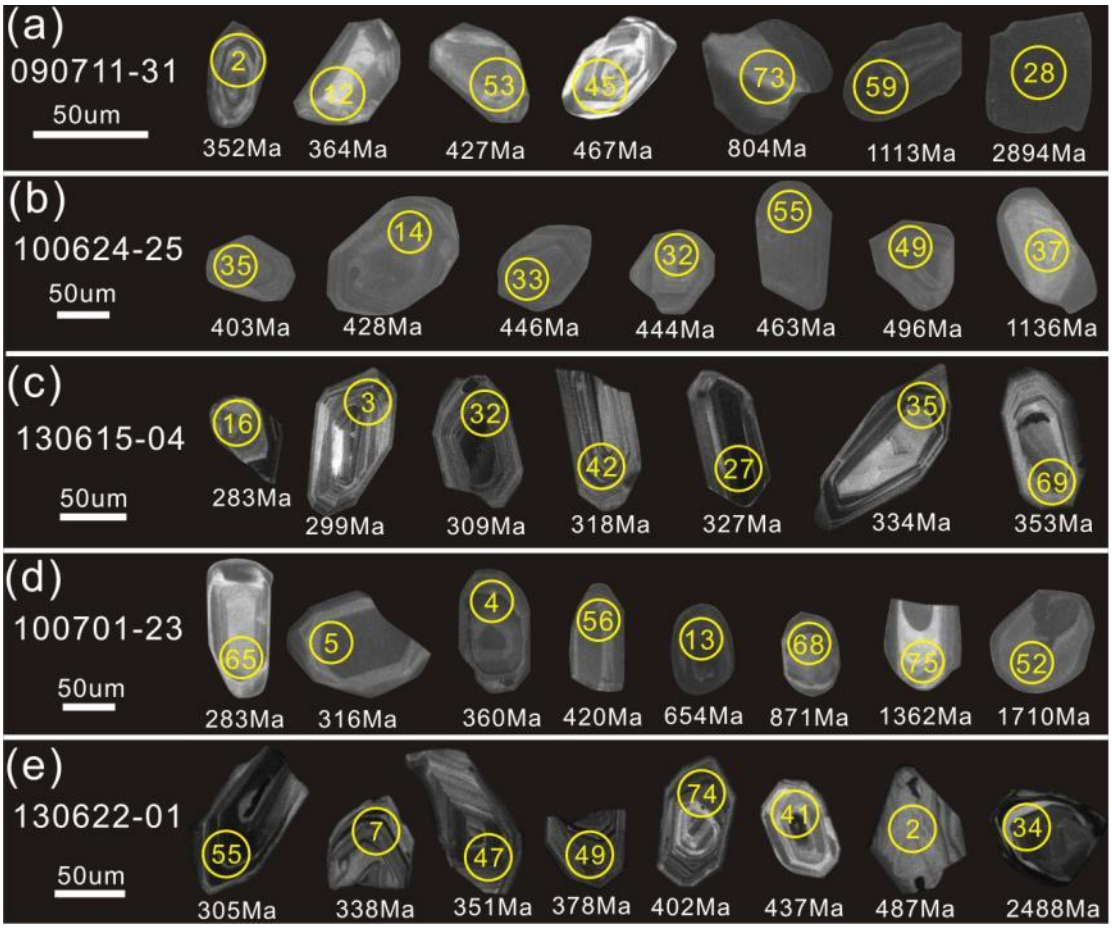

Fig. 8. Cathodoluminescence (CL) images of selected detrital zircons from each sample. The circles represent U–Pb analytical sites with numbers in the circles and ages presented below.

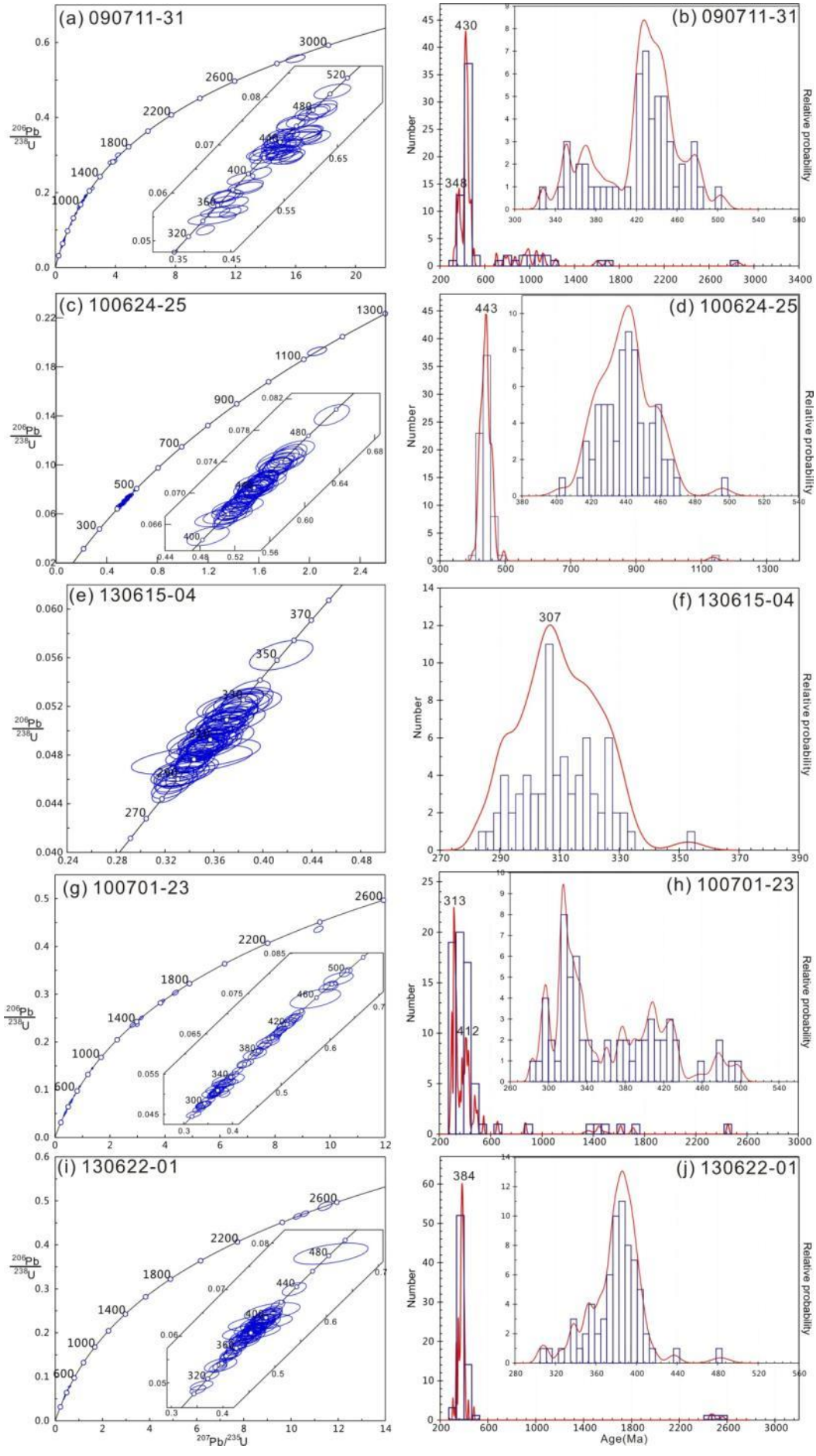
(a) 090711-31
(b) 090711-31
(c) 100624-25
(d) 100624-25
(e) 130615-04
(f) 130615-04
(g) 100701-23
(h) 100701-23
(i) 130622-01
(j) 130622-01
$^{206}Pb/^{238}U$
$^{207}Pb/^{235}U$
Number
Relative probability
Age(Ma)

Fig. 9. U–Pb concordia and probability diagrams of zircon ages of the five sandstone in this study. The inset figures within each U-Pb Concordia diagram show zircon grains with ages of 250-500 Ma.

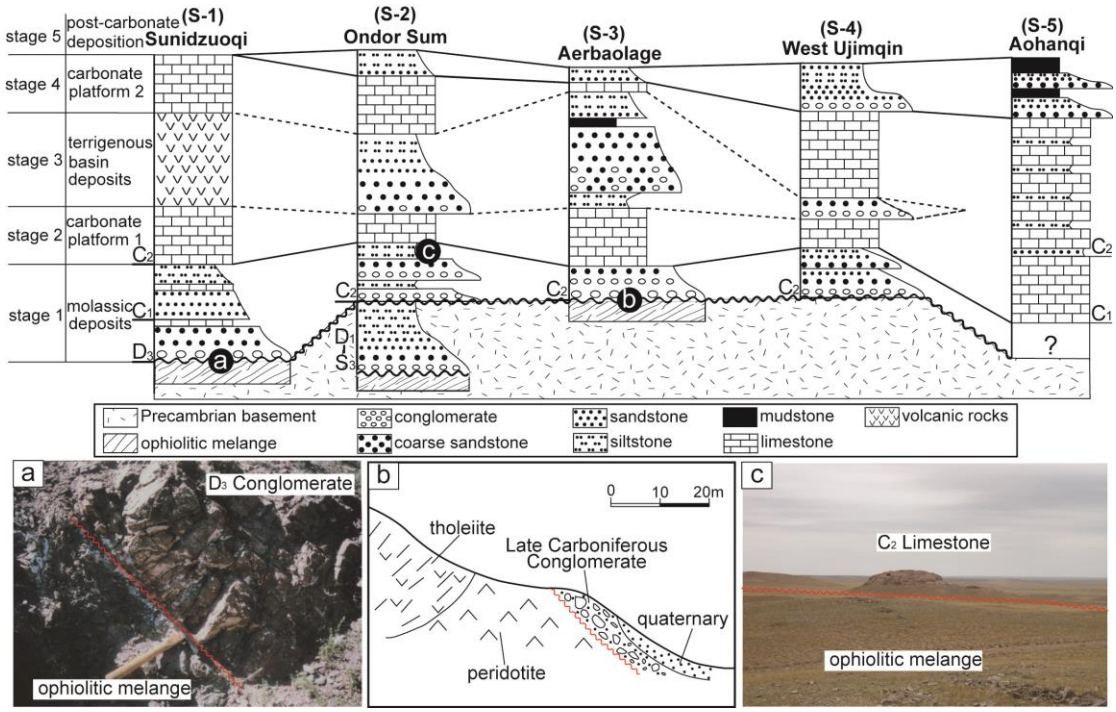

Fig. 10. Tentative correlation diagram for the five sections analyzed in this study. See Figure 1b for locations of each section. Correlations were established by tracing similar beds in the field. Five sedimentary stages were distinguished according to different rock assemblages and sedimentary facies. a: Unconformity between Upper Devonian conglomerate and ophiolitic mélange in Sunidzuoqi (from Xu et al., 2013); b: Unconformity between Upper Carboniferous conglomerate and ophiolite in Aerbaolage (from Zhang et al., 2012); c: Unconformity between Upper Carboniferous limestone and ophiolitic mélange in Ondor Sum.

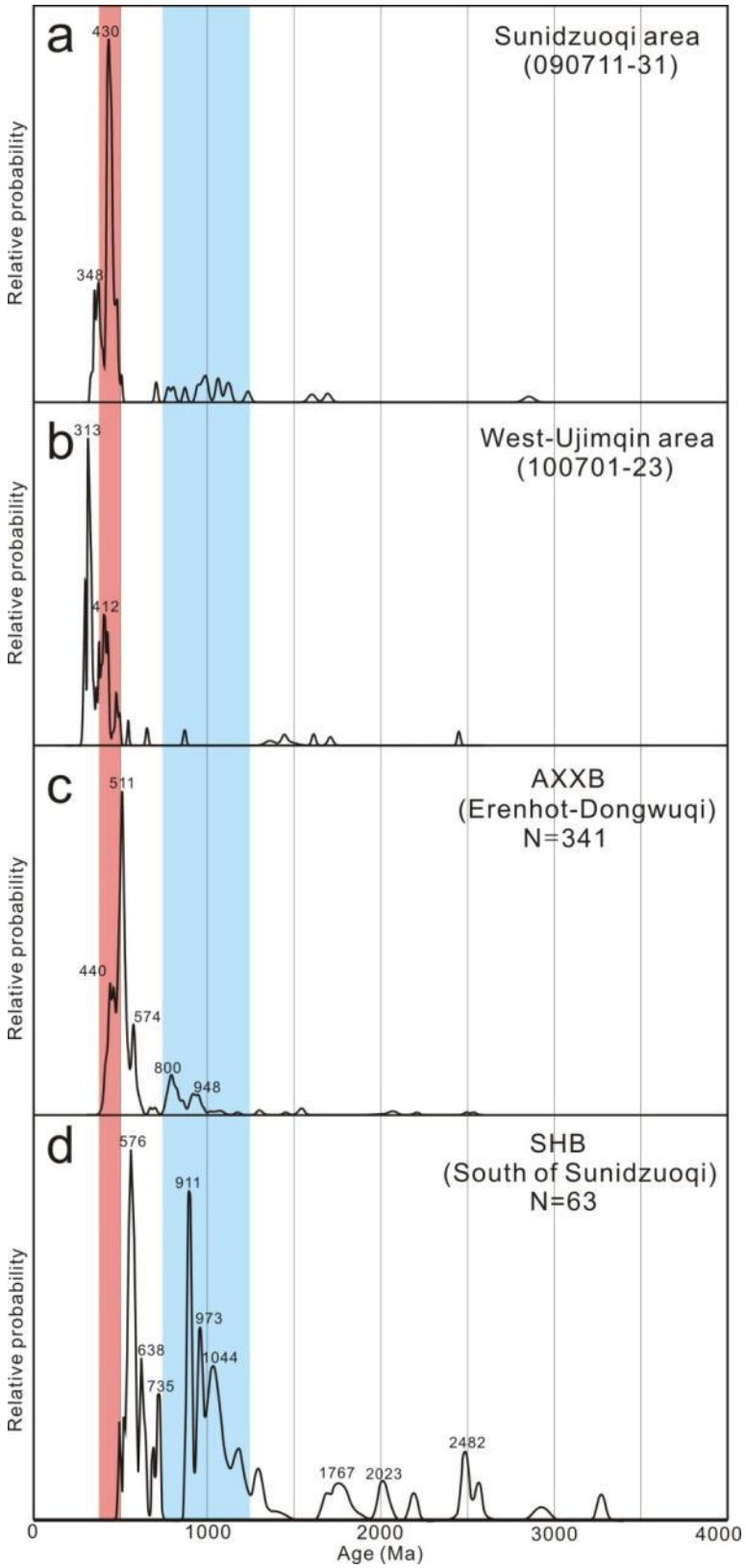

Fig. 11. Comparison of probability plots for our Carboniferous data from Sunidzuoqi (a) and West-Ujimqin (b) with the Early Paleozoic data from Airgin Sum-Xilinhot-Xing'an Block (AXXB) (c; Zhao et al., under review) and Songliao-Hunshandake Block (SHB) (d; Xu et al., 2013).

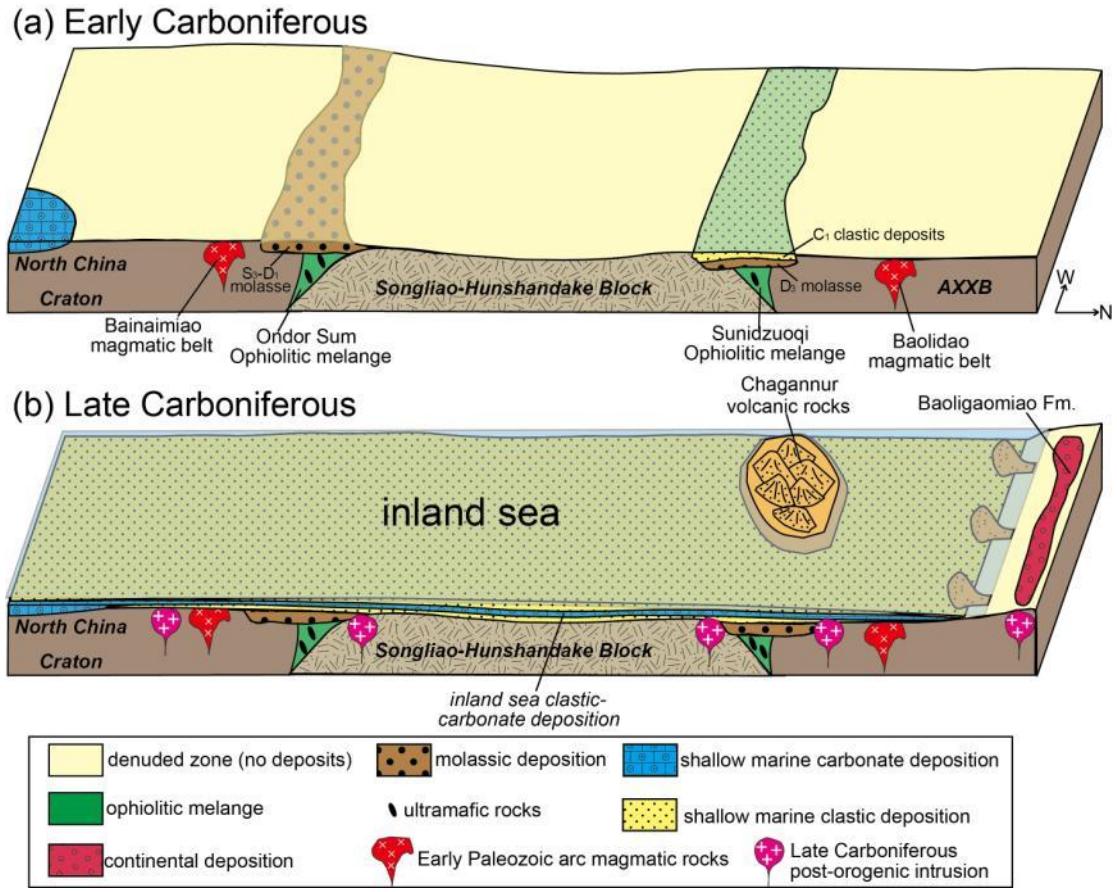

Fig. 12 Schematic evolutionary model between North China Block, Songliao-Hunshandake Block and Airgin Sum-Xilinhot-Xing'an Block (AXXB) during Carboniferous. Detailed interpretation is discussed in the text.